Imperial College
London

Carbon dioxide Storage Potential in the North Sea

Nalinee Chamwudhiprecha, Imperial College London

Abstract

The feasibility of Carbon dioxide (CO_2) injection into an extensive aquifer in the North Sea is assessed. A number of aquifer properties and operational parameters including seal permeability, horizontal permeability, perforation interval, number of wells, aquifer size and cap rock size are studied. A compositional numerical simulation is performed in the period of 50 years (30 years of injection period and 20 years of post-injection period). Initially, injection rate and number of wells are studied in order to define the injection capability of the base case aquifer. Then, by targeting the injection rate to be equivalent to the amount of CO_2 emitted from a large power station in the UK, 10 Mtonnes/year, appropriate aquifer dimensions, cap rock size and horizontal permeability are delineated. In terms of operational constraints, perforation policy is studied in order to optimize the underground distribution of gas. By focusing on the important goal of maintaining storage security, pressure response, CO_2 phase distribution and CO_2 distribution at the injector are observed. Pressure response is observed in the form of field pressure increase and average bottomhole pressure to study the effect on pressure build-up and injectivity, respectively. In order to avoid geomechanical fracturing which could lead to the escape of CO_2, feasible schemes are determined based on field pressure increase within the limit of 10% of the initial pressure.

The simulation results show that there is no impact of number of wells on pressure response as long as the total injection rate remains constant. However, using more wells enables CO_2 to be trapped by immobilization and dissolution while giving poor sweep efficiency. In order to achieve the target injection rate with 5 injectors, two appropriate aquifer dimensions are proposed: the area of 3,850 km^2 with the thickness of 1,260 m and the area of 11,550 km^2 with the thickness of 630 m. For the same aquifer volume, thickness plays a more important role on pressure response than area. By increasing the aquifer thickness, pressure impact can be more efficiently minimized compared to the aquifer area. Furthermore, the existence of a cap rock with appropriate size and permeability is significant in providing a structural trap. The proposed cap rock area and thickness are 1,411 km^2 and 63 m, respectively. Cap rock should at least cover the entire area of CO_2 plume in order to avoid CO_2 migration and a thicker cap rock helps minimize pressure build-up. Preferable cap rock permeability is 0.1 mD or less to prevent CO_2 leakage. In terms of pressure, high seal permeability results in both high and low pressure build-up. For completion policy, only deeper layers of the aquifer should be perforated in order to minimize pressure build-up and enhance CO_2 displacement efficiency. In terms of horizontal permeability, the value should be appropriate as high permeability can give positive impact on injectivity, but negative impact on pressure build-up, displacement efficiency and storage security.

Introduction

CO_2 emissions contribute towards the greenhouse effect and climate change (Ghanbari et al., 2006). The majority of anthropogenic CO_2 comes from power and industry sectors, for example, fossil fuel combustion (IPCC, 2005). Carbon Capture and Storage or CCS has aroused considerable interest because it is a way of reducing these emissions (Holloway et al., 2006). Various geological sites are considered suitable for storage in CCS, including depleted oil and gas reservoirs, deep saline aquifers and deep unminable coal seams (Gale, 2004). In the past, the main interest of CO_2 injection relied on oil or gas reservoirs as an enhanced oil recovery (EOR) technique where CO_2 and the remaining oil in place become miscible and the oil can therefore be extracted from the reservoir. However, saline aquifers are currently considered as potential sequestration sites since they have a large estimated capacity and wide distribution throughout the globe (Gale, 2004, Nicot, 2008). Saline aquifer sequestration was first mentioned in 1992 (Van der Meer, 1992) and currently, there are several successful projects of aquifer injection, for example, Sleipner (Norway), In Salah (Algeria), Ketzin (Germany), and K12B (Netherlands) which prove the feasibility of this emerging storage option. The first attempt of CO_2 injection into saline aquifer occurred in 1996 when 1 Mtonnes of CO_2 is annually injected into a shallow underground aquifer in the North Sea, known as the Sleipner project (Baklid et al., 1996). However, saline aquifer storage may cause several problems including migration into groundwater leading to contamination (Gale, 2004) and risk of overpressure, causing fracturing and possible leakage due to its shallow position. Pressure build-up is also one of the associated risks for aquifer storage, as large amounts of fluid are added without any removal. This could eventually induce fracturing or aquifer deformation which negatively impacts storage security.

Four types of trapping mechanisms occur at different timescales when CO_2 is sequestered; structural trapping, residual trapping, solubility trapping and mineralization. Structural trapping involves capturing the majority of injected CO_2 in the form of mobile gas beneath structural or stratigraphic traps, seal integrity is therefore the most significant factor in determining the storage security for both short and long term (Kumar et al., 2004; Ngheim, 2009). However, the risk of this storage method is the highest due to the uncertainties of the field characteristics and and relating geomechanic effects. Residual trapping occurs when CO_2 is trapped in the pore space as an immobile phase by taking the advantage of the capillary and wettability effects (Gale, 2004; Ngheim et al., 2009). This process occurs when brine starts invading the CO_2 plume and traps the supercritical CO_2 in the pores space (Kumar et al., 2004). Capillary trapping is considered as the most rapid trapping mechanism (Qi et al., 2009). Also, as CO_2 is highly soluble in brine, solubility trapping can occur (Ngheim et al., 2009). The degree of CO_2

solubility depends on several factors including salinity, temperature and pressure. When there is a drop in pressure, CO_2 can come out of solution leading to further migration. Solubility and residual trapping are considered as safe storage mechanisms as the risk of leakage does not depend directly on the integrity of the cap rock (Suekane, 2007). CO_2 can also react with solid minerals present in formation water and form precipitates, which considered as the ultimate desirable method of storage due to its long-term integrity. However, mineralization is not considered in this study as it takes up to hundreds or thousands of years to yield a reasonable amount due to the slow kinetics of precipitation reactions and also the capacity of CO_2 stored by this method is relatively small compared to residual trapping or mobile gas (Kumar et al., 2004).

In order for saline aquifers to be potential storage sites, they must have the following properties: size, porosity and permeability and depth (Bentham & Kirby, 2005). The North Sea is theoretically considered as one of the most effective storage sites according to the existence of several sedimentary basins, for instance, the Inner Moray Firth basin and the Bunter Sandstone, which contain very large volumes of saline water-bearing reservoir rocks (Holloway et al., 2006). A number of simulation studies have been carried out focusing on widely different aspects using different kinds of simulators e.g. Pruess et al., 2003; Kumar et al., 2004; Mo & Akervoll, 2005; Qi et al., 2007; Kartikasurja et al., 2008; Primera et al., 2009; Sifuentes et al., 2009; Nghiem et al., 2009; Vandeweijer et al., 2009. However, a limited amount of research has been focused on the impact on pressure response. Van der Meer (1992) first suggested the idea of the injection limitation due to an increase in pore pressure. Van der Meer et al. (2006) emphasized the effect of injecting additional fluid into an aquifer on fluid volumes and pressures in the total storage system by focusing on CO_2 that dissolves in water. Yang (2008) proposed that rapid pressure build-up during injection greatly limited storage volume for a closed system and in order to relieve the injection pressure and the storage capacity, brine could be produced from the reservoir. Birkholzer et al. (2009) investigated the region of influence from CO_2 injection in terms of brine displacement and pressure perturbation. Oruganti and Bryant (2009) studied the effect of the existence of sealing faults towards pressure build-up.

This paper assesses the feasibility of CO_2 injection into an extensively large aquifer in the North Sea by aiming at the important goal of increasing storage security. Aquifer properties and operational constraints, including seal permeability, horizontal permeability, perforation interval, number of wells, aquifer size and cap rock size are studied by focusing on field pressure response, well injectivity and CO_2 distribution.

Numerical Simulations

Numerical simulations are performed using the compositional Eclipse E300 software. A base case model is constructed by using aquifer dimensions and properties from an existing aquifer in the North Sea, the Bunter Sandstone (Bentham, 2006). The model is assumed to be homogeneous. Initially, injection rate and number of wells are studied in order to define the injection capability of this aquifer. By considering the target injection rate to be 10 Mtonnes/year (10^{10} kg/year) which corresponds to the estimation of CO_2 emission rate from large power stations, supplying 1-3 GW of coal-powered electricity, in the UK, for example, West Burton Power Station or Ratcliffe on Soar Power Station (Holloway, 2006). However, the simulation results will show that the base case aquifer is not sufficiently large to provide the planned storage capacity. Aquifer dimensions are therefore varied and delineated based on the properties of Bunter Sandstone to allow enough storage volume. As cap rock is one of the most significant factors for a potential storage site, cap rock size and permeability are studied to justify the appropriate thickness, area and permeability. Also, aquifer permeability is varied in order to determine the appropriate value to store the planned volume without negatively affecting aquifer pressure. In terms of operational constraints, perforation interval is studied in order to optimize CO_2 underground distribution.

For every case, the injection strategy is controlled by injection rate instead of bottomhole pressure in order to reach the planned total storage with a plateau injection rate. The simulation period is 50 years including 30 years of pure CO_2 injection period and 20 years of post-injection. Pressure response, CO_2 leakage and CO_2 phase distribution are observed. Pressure response is observed in the form of field pressure increase and average bottomhole pressure to study the effect on pressure build-up and injectivity, respectively. Field pressure increase is calculated by considering the percentage difference between the maximum field average pressure occurring at any time during the simulation period and the average initial pressure of the field. In practical operations, field pressure has to be controlled not to exceed fracture pressure which could cause CO_2 migration out of the storage site. Values for the fracture-closure pressure gradients are site-specific and can be determined from direct or indirect testing, or by formation-specific default values (Zhou, 2008). For the study in this paper, feasible schemes are determined based on field pressure increase within the limit of 10% of the initial pressure. Also, CO_2 phase distribution and CO_2 distribution around the injector are observed in order to assess the security of the storage over time. Overall, generic dimensions and properties of a saline aquifer that is capable of supporting the target CO_2 storage are provided.

Model Description

A homogeneous box-shaped model of 215,600 grid cells is constructed as a base case to represent a laterally extensive aquifer. Compartmentalization is not considered in order to allow fluid transmission without excessive pressure increase. As CO_2 injected in an unconfined aquifer, it will likely disperse over a large area and in low concentrations over time (Bentham, 2005). The aquifer thickness is 126 m with an overlying seal which forms the first layer of the model. The seal layer has low permeability and high capillary entry pressure to enable CO_2 trapping. The model size and properties are gathered from the Bunter Sandstone which proves to have high storage potential amongst the reservoir rocks of the Southern North Sea (Holloway et al., 2006). In terms of perforation policy, half of the aquifer layers are completed. The input parameters for the

base case simulation are shown in Table 1.

Relative permeability curves are based on experimental data of supercritical CO_2-brine at in-situ conditions of the Viking Formation sandstone, Alberta, Canada (Bennion & Bachu, 2006). Hysteresis effects are taken into account by using both drainage and imbibition curves. Drainage occurs at the leading edge of the CO_2 plume where gas displaces water, while at the trailing edge water displaces gas in an imbibition process (Juanes et al., 2006). By using both curves, the residual trapping mechanism is activated. Relative permeability curves are shown in Figure 1. Also, a reversal of the drainage is taken into account by calculating a scanning curve with Killough's method (1976). Capillary pressure is calculated by the method of Van Genuchten (1980). Capillary pressure for seal layer is scaled with permeability by the use of the Leverett J-function.

Parameter	Value
Grid cells (i, j, k)	140 ×110 × 14
Grid block size	500 m × 500 m × 9 m
Aquifer volume	485 km^3
Porosity	0.18
Kv/Kh ratio	0.1
Kh	500 mD
Temperature	62.8 ◦C
Top depth	1717 m
Rock compressibility	1.5E-5 bar^{-1}
Pressure at 3200 m	225 bars

Table 1 - List of aquifer properties for the base case.

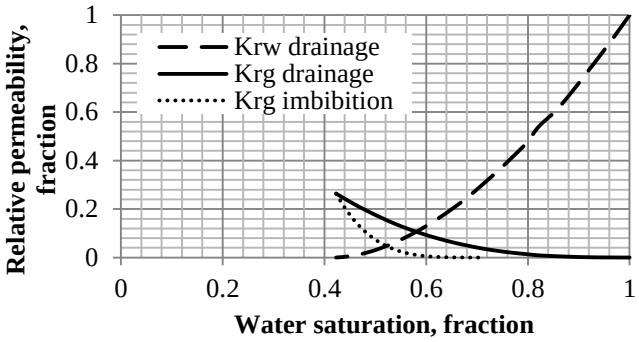

Figure 1 - Relative permeability curves (Bennion & Bachu, 2006).

Fluid Properties

CO_2 has a critical pressure of 73.8 bars and a critical temperature of 304.2 K and is a supercritical fluid at aquifer conditions (Ngheim et al., 2009). Two phases are considered in the simulation studies: a CO_2-rich phase (gas phase), and an H_2O-rich phase (liquid phase). Three compositions are included: CO_2, H_2O and NaCl while salts are assumed to be in the liquid phase only. By the use of CO2STORE function, mutual solubilities of both CO_2 in water and water in CO_2 are calculated to include the effect of chloride salts in the aqueous phase (Spycher & Pruess, 2005). An accurate prediction of the aqueous phase density is another important aspect for modeling CO_2 storage in saline aquifers (Nghiem et al., 2009). Gas density is calculated by a cubic equation of state. Brine density is first approximated by pure water density using the method presented by Kell & Whalley (1975) and then the effects of salt and CO_2 are corrected by using the Ezrokhi's method (Zaytsev & Aseyev, 1993). The CO_2 gas viscosity is calculated using methods of Vesovic et al. (1990) and Fenghour et al. (1999). Formation brine salinity is assumed to be constant throughout the aquifer at 175,000 ppm.

Results

CO_2 Injection Rate and Number of Injectors

The study initially aims at the optimum injection rate per well in order to evaluate the amount of CO_2 that can practically be stored in the base case model. For every case, only half of the aquifer layers are perforated. By varing the injection rate, the pressure response is observed. The results in Table 2 show that in order to maintain the field pressure not to exceed 10 % of its original value, only 440,000 tonnes/year of CO_2 can be injected into this base case model by using one well. Furthermore, if the planned injection rate of 10 Mtonnes/year is to be injected, the pressure will greatly increase nearly 100%. Therefore, in order to reach the target injection rate, either many wells or a larger aquifer has to be used.

Case No.	Injection rate		Field pressure increase
	m^3/day	tonnes/year	
1	34,250	23,000	0.5 %
2	148,000	100,000	2.3 %
3	650,000	440,000	10.0 %
4	700,000	473,000	10.7 %
5	800,000	540,000	12.1 %
6	1,000,000	675,000	14.0 %
7	2,070,000	1,400,000	20.0 %
8	2,960,000	2,000,000	30.0 %
9	15,000,000	10,000,000	96.4 %

Table 2 - Results of field pressure increase from injection rate variation.

Moreover, in order to assess the feasibility of injection, appropriate number of wells to be used is identified. Total injection rate is fixed at 10 Mtonnes/year while the injection rate per well varies for different cases. By using a variation of number of injectors into 1 well, 3 wells, 5 wells, 7 wells and 9 wells, CO_2 is injected into the base case model. Well locations are shown in Figure 2.

The results (Table 3) show that the number of wells does not have a significant effect on field pressure. Allowing more wells to be used does not lower pressure buildup as the total injection rate remains equal for all the cases. However, the number wells used affect the storage mechanisms as shown in Figure 3. A larger number of wells lead to more immobile and dissolved CO_2, hence less mobile CO_2. As more wells are used, there is more contact area between CO_2 and water which enhances the rate of dissolution and capillary trapping. The rate of dissolution depends on the amount of mixing of CO_2 and

formation water (Kumar et al., 2004). In terms of CO_2 distribution, for every case, CO_2 tends to accumulate around the wellbore along the injection period, then gradually spreads out to form a gas layer below the overlying seal after the injection ceases. Figure 4 shows CO_2 distribution at the injector for plume radius comparison. For the case with 1 well, CO_2 is forced to be injected at high injection rate which leads to wider plume radius. For the case with more wells, CO_2 tends to accumulate and concentrate around the wellbore and water is not entirely swept in the lower layers. The high rate in the single-well system makes gravity forces relatively small which enhances sweep efficiency, while in multiple well scenarios, low rates allow time for the CO_2 to accumulate at the top of the formation.

In conclusion, a sufficient number of wells should be used in order to optimize both the storage mechanism by enhancing both the immobile and solubility trapping, and the sweep efficiency. However, it is not feasible to inject 10 Mtonnes/year into the base case aquifer even with more wells as pressure build-up exceeds the 10 % limit of fracture prevention. Therefore, the remaining option is choose a larger aquifer.

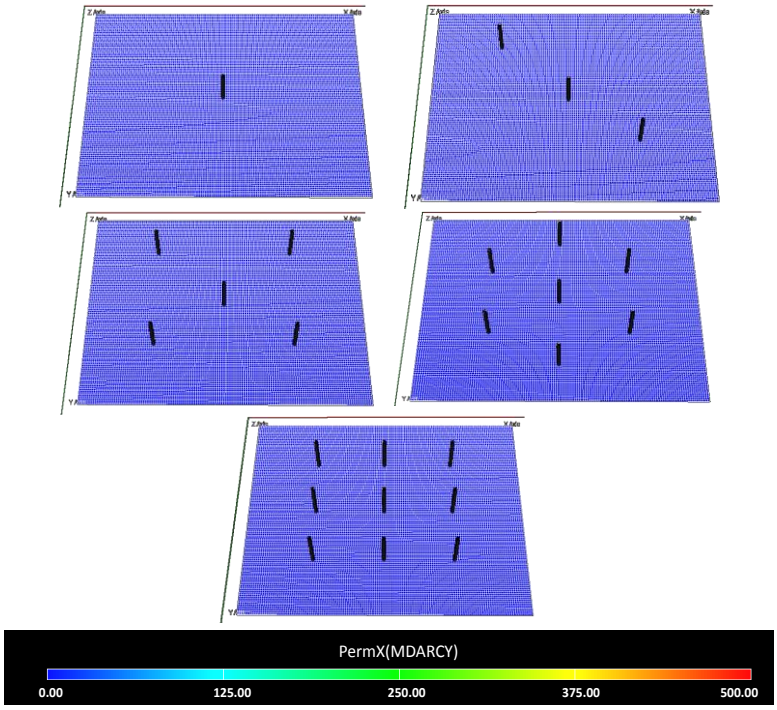

Figure 2 - 2D top view of the base case model showing well locations for each case.

Case No.	No. of wells	Injection rate per well		Field pressure increase
		m^3/day	Mtonnes/year	
1	1 well	15,000,000	10	96.4 %
2	3 wells	5,000,000	3.5	103.9 %
3	5 wells	2,960,000	2	102.6 %
4	7 wells	2,150,000	1.5	103.7 %
5	9 wells	1,670,000	1.1	103.3 %

Table 3 - Injection rate for cases with number of wells variation.

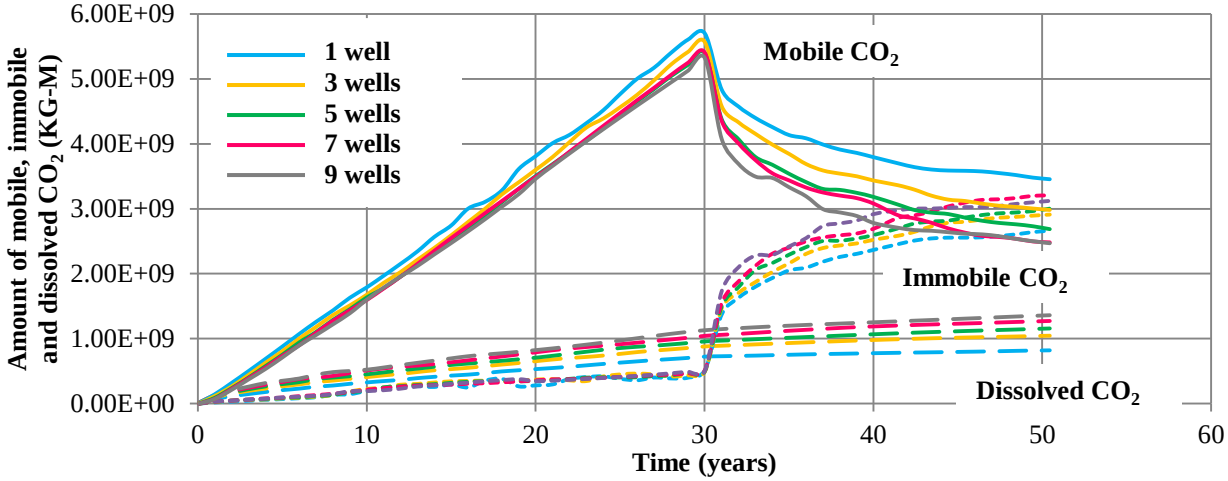

Figure 3 - Results of injected CO_2 in different phases for different numbers of injection wells.

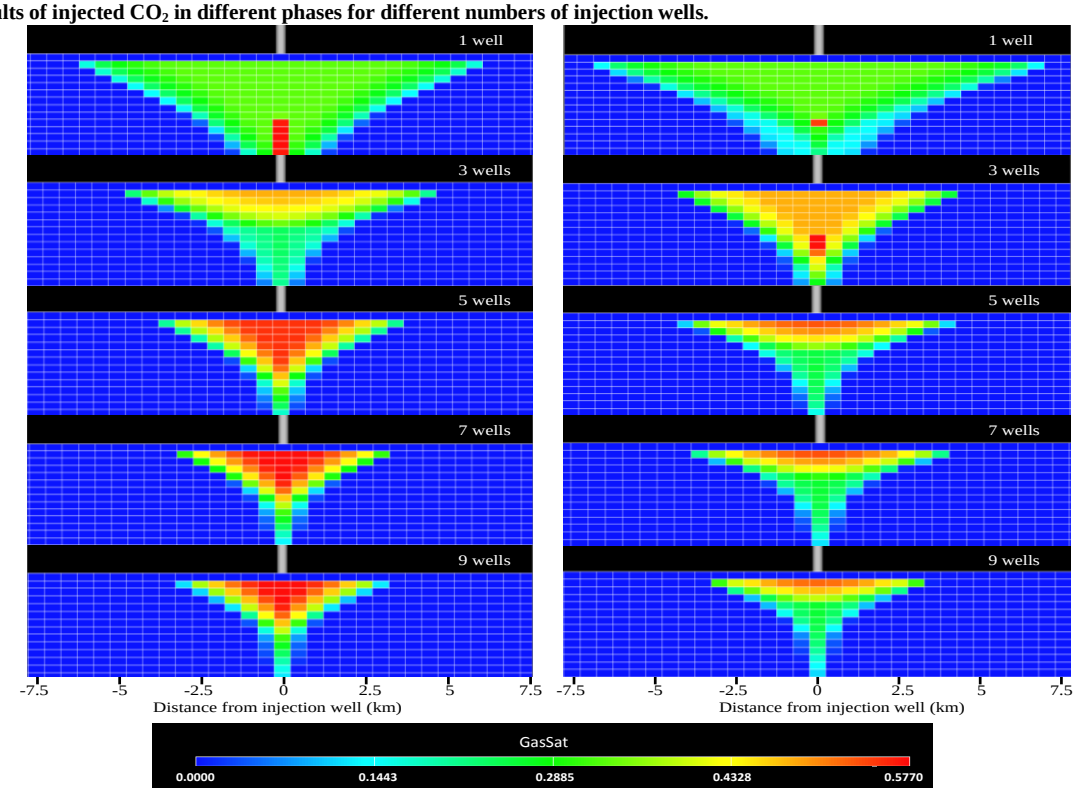

Figure 4 - 2D cross-section view of CO_2 distribution at the injector for different numbers of wells *Left: at the end of the injection period (30 years) Right: at the end of the simulation period (50 years) Top to bottom: no. of wells 1, 3, 5, 7, 9.*

Aquifer Dimensions

In order to practically store the planned CO_2, the aquifer must be sufficiently large in order to accommodate the storage volume and overcome the limitations on pressure increase. According to the previous study of the injection rate, the base case aquifer is not capable of storing the planned storage volume. Therefore, the base case aquifer model is enlarged with the same properties by using five injectors with the total injection rate of 10 Mtonnes/year. Two means of investigating the size of the aquifer are used: controlling lateral area and varying thickness and controlling thickness and varying lateral area. For both cases, appropriate area and thickness are determined by observing the average field pressure to increase within the limit of 10%.

For the first case, controlling area and varying thickness, the area is fixed at 3,850 km^2 according to Bunter Sandstone aquifer's dimensions (Bentham, 2006). The base thickness value is 126 m, according to Bunter Sandstone aquifer's dimensions (Bentham, 2006), which is multiplied with 3, 5, 7, 9 and 10. According to the results of field pressure (Table 4) , it can be observed that the thickness of 1,260 m (10 times of the base thickness value) gives a pressure increase within the limit of 10% as thick aquifers allow pressure to dissipate more vertically and hence alleviate pressure build-up. Considering the bottomhole pressure, the case with the thickness of 126 m gives the highest bottomhole pressure, in other words, the lowest injectivity owing to the difficulty of the injection into a thin aquifer while the other cases show relatively similar bottomhole pressure. Therefore, if the aquifer thickness is sufficiently large, there will be no effect on injectivity. In terms of phase

distribution, in the case with high value of thickness, CO_2 tends to be less mobile and more dissolved in water as seen in figure 5. Thicker aquifers lead to more contact area between CO_2 and water which enhances the rate of dissolution. Also, longer distance of migration enables water to trap CO_2 which results in higher residual gas. The results also correspond to the previous study stating that the transition of CO_2 from the free gas phase into the dissolved phase in water has a pressure-reducing effect (Van der Meer & Van Wees, 2006); this is because the effective density of CO_2 in brine is much higher than its own phase. Considering the CO_2 plume radius, the case with higher value of thickness gives narrower plume radius as CO_2 is trapped as an immobile phase before reaching the top of the aquifer as seen in Figure 6. Areal displacement is greatly efficient for the case with the thickness of 126 m while other cases show similar results.

Case No.	Thickness	Thickness	Field pressure increase	Average bottomhole pressure (Bars)
1	Thickness × 1	126 m	102.6 %	152
2	Thickness × 3	375 m	39.4 %	127
3	Thickness × 5	630 m	23.6 %	124
4	Thickness × 7	882 m	15.6 %	125
5	Thickness × 9	1,134 m	11.3 %	125
6	Thickness × 10	1,260 m	9.6 %	126

Table 4 - Results of pressure increase and average bottomhole pressure from aquifer thickness variation.

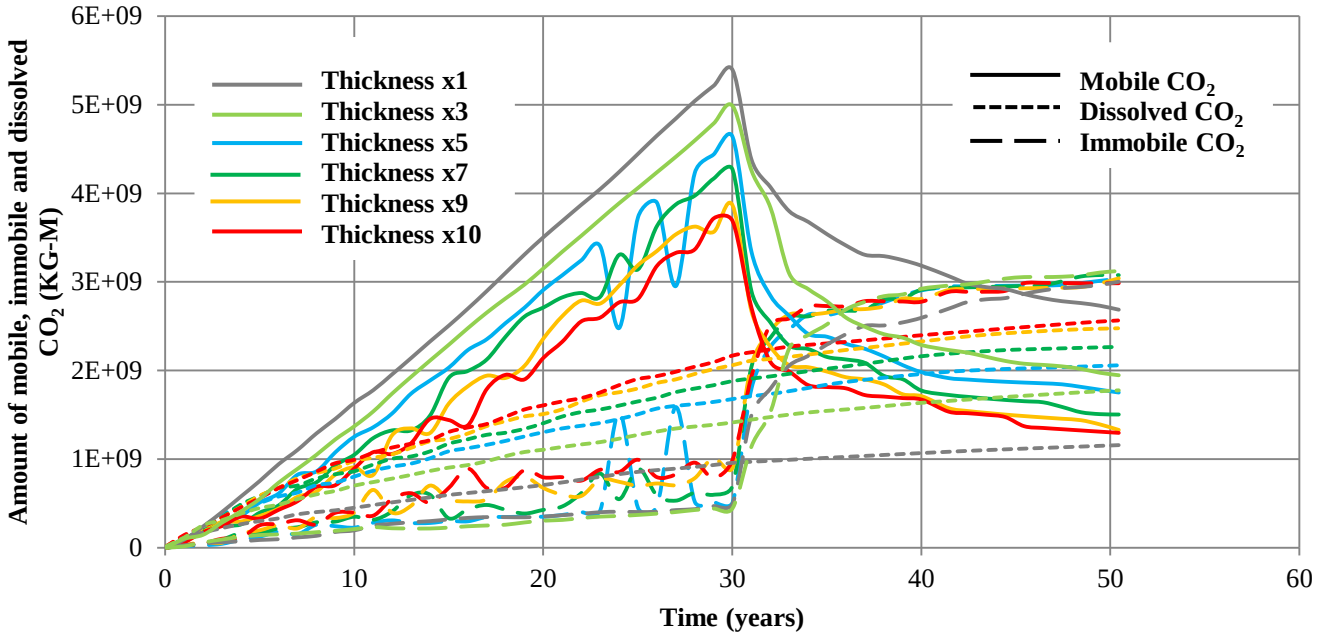

Figure 5 - Results of injected CO_2 in different phases from aquifer thickness variation.

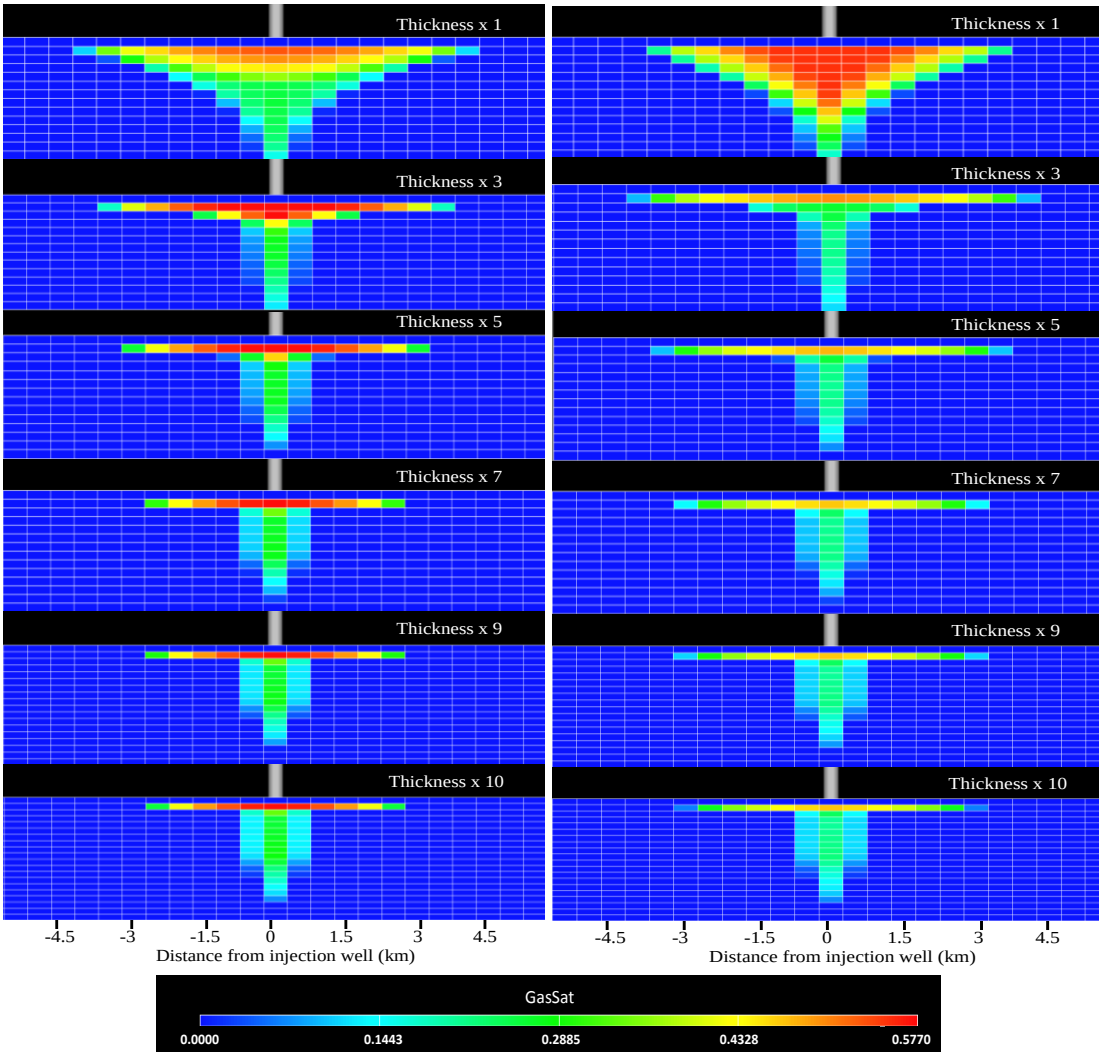

Figure 6 - 2D cross-section view of CO_2 distribution at the injector from thickness variation *Left: at the end of the injection period (30 years) Right: at the end of the simulation period (50 years) Top to bottom: Thickness ×1, ×3, ×5, ×7, ×9, ×10.*

For the case that the aquifer thickness is controlled while the area is varied, the thickness is fixed to be 5 times of the base thickness value, 630 m, three different sizes of aquifer were studied:- 2 times, 2.5 times and 3 times of the base area value (3,850 km^2). It can be concluded that with the given thickness of 630 m, the appropriate area is 11,550 km^2 (3 times of the base area value) as field pressure increase does not exceed the control limit. The results of pressure increase and average bottomhole pressure are shown in Table 5. Large aquifers can withstand higher overall pressure build-up and also contributes to higher injectivity as pressure is allowed to disperse throughout a larger area. Lower bottomhole pressure is observed in the case with larger area which results in higher injectivity. However, there is no significant difference on phase distribution as the contact area remains the same for all cases. Also, the results show no significant difference on CO_2 underground distribution.

Case No.	Area	Area	Field pressure increase	Average bottomhole pressure (Bars)
1	Area ×1	3,850 km^2	23.6 %	124
2	Area × 2	7,700 km^2	13.6 %	120
3	Area × 2.5	9,625 km^2	10.9 %	119
4	Area × 3	11,550 km^2	10.0 %	118

Table 5 - Results of pressure increase from aquifer area variation.

Finally, the effect of thickness and area are compared by fixing the volume of the aquifer to be 4,851 km^3 and vary the aquifer thickness and area. By maintaining the volume, the results show that thickness plays a more important role on pressure response than area according to table 6. In other words, for the same value of aquifer volume, the aquifer with larger thickness value gives lower pressure increase. In terms of CO_2 distribution, gas tends to be stored more vertically in the case with higher thickness which leads to narrower plume radius as shown in Figure 7. Also, CO_2 phase distribution is shown in Figure 8. More immobile gas and less mobile gas are present in the case with higher thickness value. However, there is no difference in the

amount of gas dissolved in water. Therefore, the aquifer thickness is one of the most important criteria when determining a suitable storage site so as to minimize the pressure effect together with increasing the amount of trapped gas.

Case No.	Thickness & area	Area	Thickness	Volume	Field pressure increase
1	Thickness×1 Area×1	3,850 km^2	126 m	485.1 km^3	102.6 %
2	Thickness×10 Area×1	3,850 km^2	1,260 m	4,851 km^3	9.6%
3	Thickness×5 Area×2	7,700 km^2	630 m	4,851 km^3	13.6%

Table 6 - Properties and results from aquifer thickness and variation.

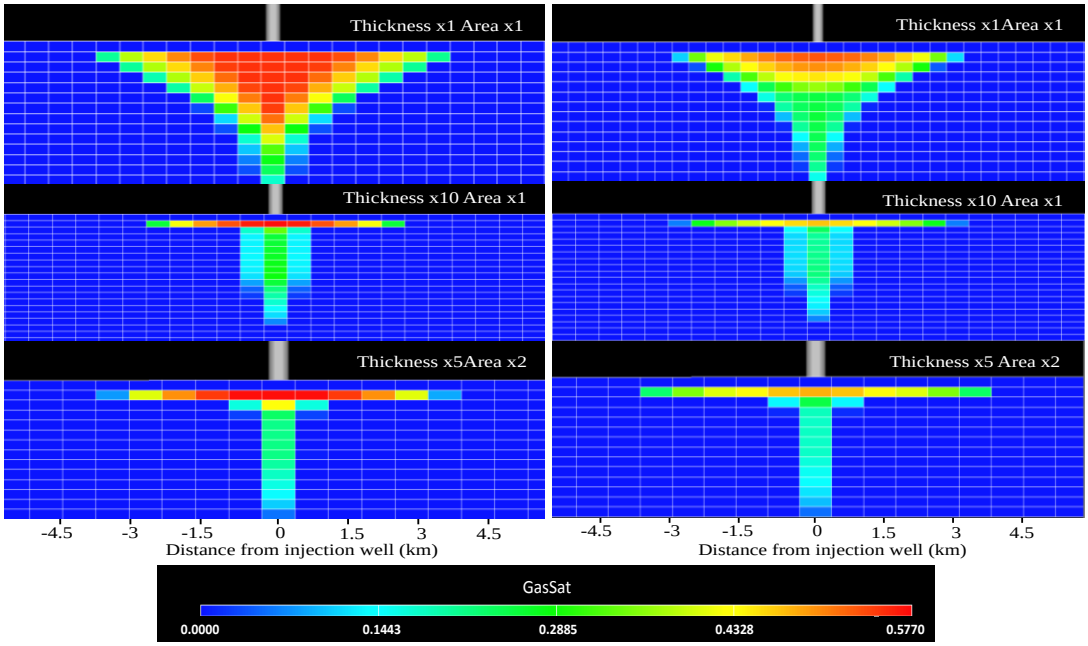

Figure 7 - CO_2 distribution at the injector from area and thickness variation *Left: at the end of the injection period (30 years) Right: at the end of the simulation period (50 years) Top to bottom: Thickness x1 Area x1, Thickness x10 Area x1, Thickness x5 Areax2.*

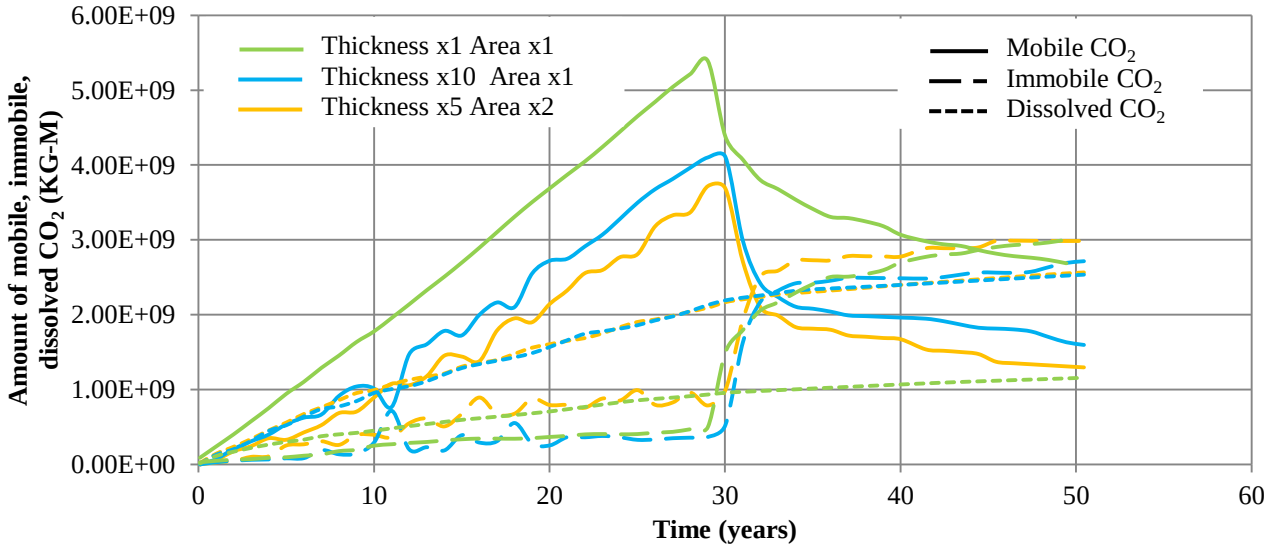

Figure 8 - Results of injected CO_2 in different phases from aquifer thickness and area variation.

In conclusion, in order to store 10 Mtonnes/year of CO_2 by using 5 wells the aquifer area should be at least 3,850 km^2 with the thickness of 1,260 m or 11,550 km^2 with the thickness of 630 m to withstand the pressure limitation. The model with the dimensions of 70 km × 55 km × 1,260 m will be used for further study of the influence of other constraints (cap rock size, perforation interval, horizontal permeability, seal permeability).

Cap rock Size

One of the most important factors for potential storage aquifers is the existence of a structural trap. A geological seal provides a vertical flow barrier to prevent buoyant CO_2 from leaving the formation (Flett et al., 2004) which could hence contaminate other sources. In abandoned hydrocarbon fields, the existence and quality of the seal is demonstrated which is normally not the case for saline aquifers (Bentham & Kirby, 2005). This paper evaluates the significance of the seal dimensions in terms of its area and thickness on pressure distribution. The study is carried out by two means: varying the area and varying the thickness of the cap rock. For all cases, seal permeability is equal to 0.001 mD. Capillary pressure for the seal layer is scaled with permeability which is important for the cap rock invasion simulations.

For the case of area variation, three different sizes of cap rock are studied; 3850 km^2 (covering all aquifer area), 1,410.5 km^2 (covering part of the CO_2 distribution) and 1,411 km^2 (covering all the CO_2 distribution). For all cases, aquifer thickness is 1,134 m with an overlying seal with a thickness of 126 m. Each cap rock size is shown in Figure 9. The results from Figure 10 show that CO_2 leakage is observed in the case which only part of the CO_2 plume is covered. Considering long-term storage, mobile CO_2 can easily find an escape path if the existing cap rock is not sufficiently large and continuous. However, the results show no difference in pressure increase for the three cases according to Table 7. As required cap rock size relies on the plume radius, the proximity between the wells also affects the required size. When the well interval is large, cap rock then needs to be large in order to cover the overall CO_2 plume and vice versa. Also, there is no significant difference on CO_2 phase distribution for all cases.

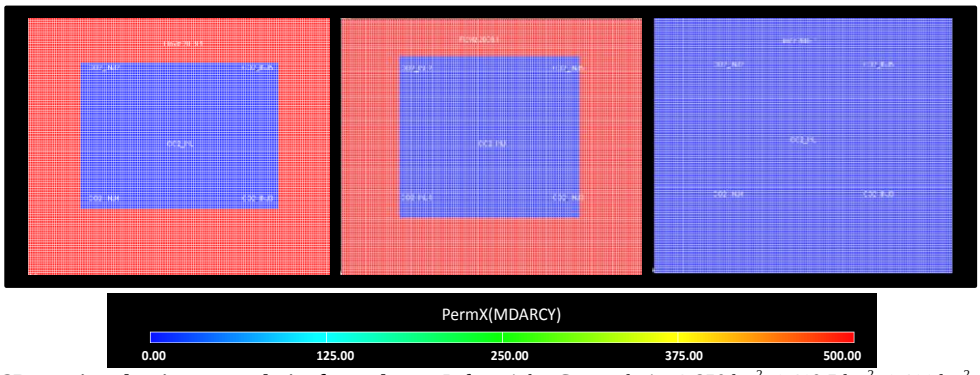

Figure 9 - 2D top view showing cap rock size for each case *Left to right: Cap rock size 3,850 km^2, 1,410.5 km^2, 1,411 km^2.*

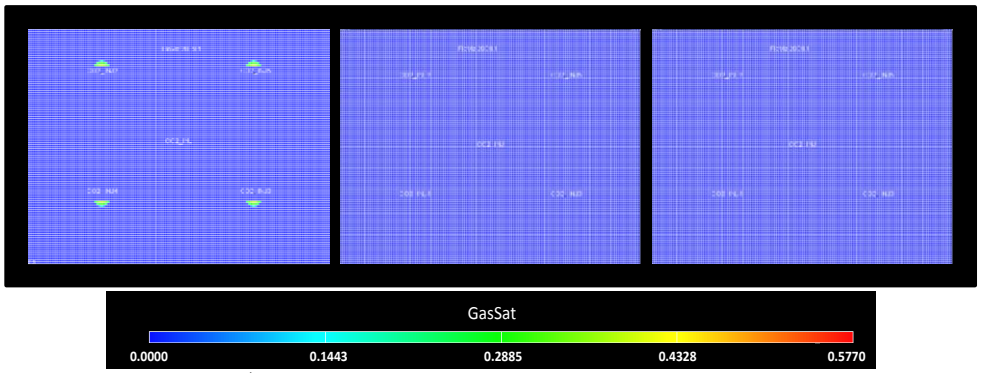

Figure 10 – CO_2 distribution of the seal layer (1st layer) of the aquifer from cap rock size variation *Left to right: Cap rock size 3,850 km^2, 1,410.5 km^2, 1,411 km^2.*

Case No.	Cap rock size	Field pressure increase
1	3,850 km^2 (covering all aquifer area)	9.6%
2	1,410.5 km^2 (covering part of the CO_2 distribution)	9.6%
3	1,411 km^2 (covering all the CO_2 distribution)	9.6%

Table 7 - Results of pressure increase from cap rock size variation.

For thickness variation, the seal area is fixed at 1,411 km^2 which covers all CO_2 plume distribution and the seal thickness is varied to be 10 m, 21 m, 42 m, 63 m and 126 m. The results from Table 8 show that thicker seal gives less effect on pressure build-up but no impact on injectivity. However, pressure response is not highly sensitive on cap rock thickness variation. Also, seal thickness does not influence on CO_2 leakage, CO_2 underground distribution or CO_2 phase distribution as there is no change in the contact area between CO_2 and brine.

Case No.	Cap rock thickness	Field pressure increase	CO_2 leakage	Average bottomhole pressure (bars)
1	126 m	9.6 %	No	126
2	63 m	9.7 %	No	126
3	42 m	10.2 %	No	126
4	21 m	10.7 %	No	126
5	10 m	11 %	No	126

Table 8 - Results of pressure response and CO_2 leakage from cap rock thickness variation.

In conclusion, cap rock area should be extensively large and cover the CO_2 plume distribution in order to avoid any migration path. Also, cap rock thickness should be sufficiently high to lower the pressure effect. The proposed dimensions of the cap rock are the area of 1,411 km^2 with the thickness of 63 m.

Seal Permeability

Cap rock integrity is one of the most important factors which helps reduce the risk of CO_2 leakage. By varying the permeability of the cap rock to be 10 mD, 1 mD, 0.5 mD, 0.1mD and 0.01 mD while maintaining the seal thickness at 126 m, gas saturation is observed in the uppermost layer (seal layer) as shown in Figure 11. The results show that CO_2 leakage is observed at the seal permeability of 0.5 mD or higher. Capillary entry pressure is dependent on permeability (pore throat size) as gas requires greater pressure to displace brine in a microscopic scale. For cases with low seal permeability, CO_2 tends to migrate horizontally and forms more lateral CO_2 plume while cases with high seal permeability CO_2 is allowed to be stored in the seal layer which results in thicker CO_2 plume. However, by observing gas distribution in the lower layers, all of the cases appear to have comparatively similar displacement efficiency. For CO_2 phase distribution, the results are inconclusive.

In terms of pressure effect, Table 9 shows inconclusive results on average field pressure increase. On one hand, a low permeability seal layer forms a pressure barrier which causes the pressure to buildup extensively higher than the case with higher permeability. On the other hand, although a low permeability seal prevents CO_2 leakage because of its high capillary pressure, it also allows a small amount of water to flow over the very large area of the cap rock which helps release the pressure build-up. Overall, seal permeability can affect field pressure response both positively and negatively. Furthermore, no effect on bottomhole pressure can be observed. The most appropriate value for seal permeability is 0.1 mD or less to prevent CO_2 from escaping and provide reasonable pressure increase.

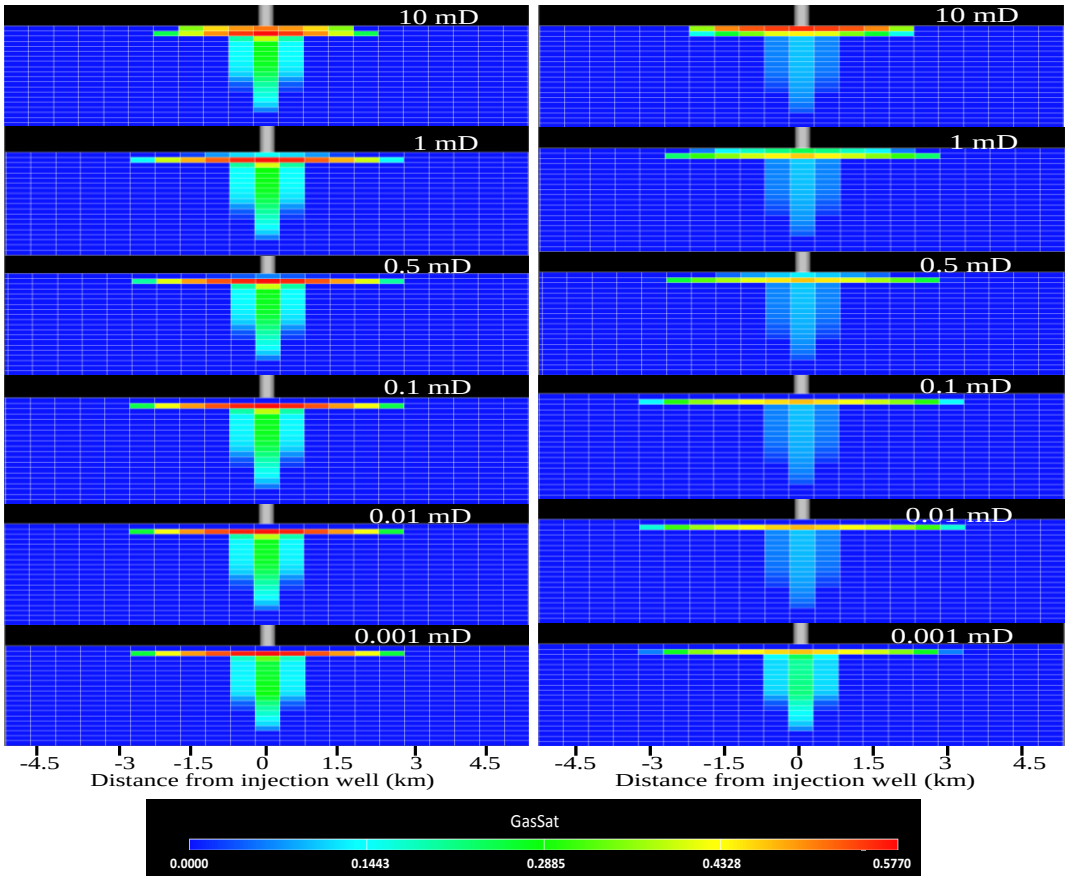

Figure 11 - Results of CO_2 migration into the seal layer from seal permeability variation *Left: at the end of the injection period (30 years) Right: at the end of the simulation period (50 years) Top to bottom: seal permeability 10 mD, 1 mD, 0.5 mD, 0.1 mD, 0.01 mD and 0.001 mD*

Case No.	Seal permeability	Field pressure increase	Average bottomhole pressure (Bars)
1	10 mD	9.7 %	126
2	1 mD	9.2%	126
3	0.5 mD	9.2 %	126
4	0.1 mD	9.6 %	126
5	0.01 mD	9.8 %	126
6	0.001 mD	9.6 %	126

Table 9 - Results of field pressure and injection pressure increase from seal permeability variation.

Perforation Interval

Different perforation intervals of injection wells are studied in order to investigate the effect on underground CO_2 distribution for storage optimization. Perforation interval is varied to be from layer 2 to 20 (all sand layers) and from layer 10 to 20 (half of the aquifer thickness). As seen in Figure 12, in the case which all the layers are perforated, gas tends to accumulate mostly in the upper layers. While in the case which half of the layers are perforated, gas is also distributed in the lower layers which enhances displacement efficiency. Comparatively larger plume radius can be observed in the case which all of the layers are perforated. CO_2 phase distribution (Figure 13) shows that gas is preferably stored as an immobile phase in the case which half of the layers are perforated but less gas is in a dissolved phase.

In terms of pressure build-up, lower pressure increase is observed in the case which only half of the aquifer thickness is perforated as shown in Table 10. As gas is also stored in lower layers, it is trapped before reaching the upper layers which increases the rate of immobilization. This also results in less field pressure build-up. In terms of injectivity, higher bottomhole pressure is observed when only half of the layers are perforated which lowers injectivity. This is due to the fact that the same amount of CO_2 has to be injected through less perforated area. Therefore, in order to optimize the storage capacity and sweep efficiency with less pressure build-up, only deeper parts of the aquifer should be perforated.

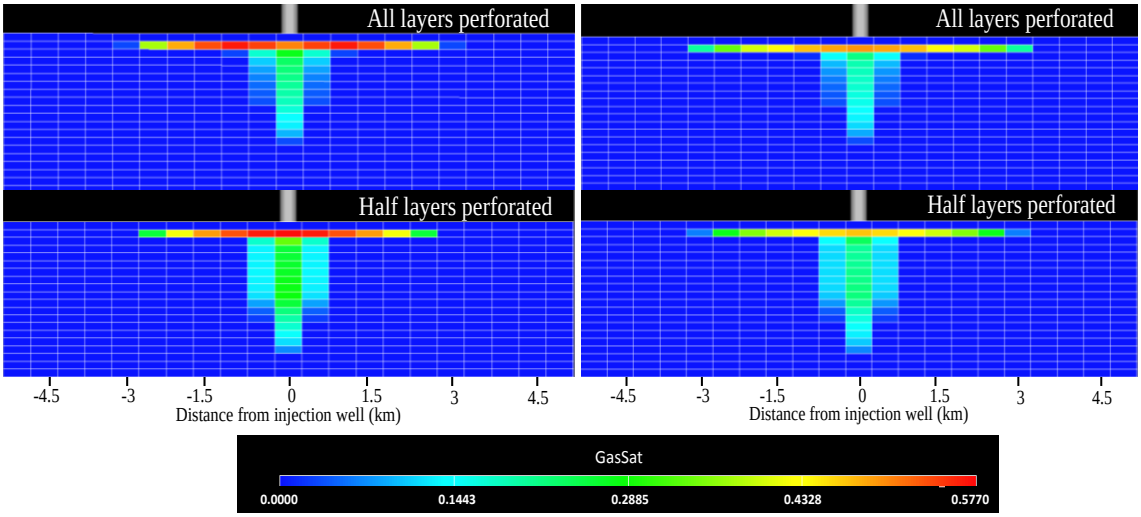

Figure 12 - CO_2 distribution at the injector from perforation interval variation *Left: at the end of the injection period (30 years) Right: at the end of the simulation period (50 years) Top: layer 2 to 20 perforated Bottom: layer 10 to 20 perforated*.

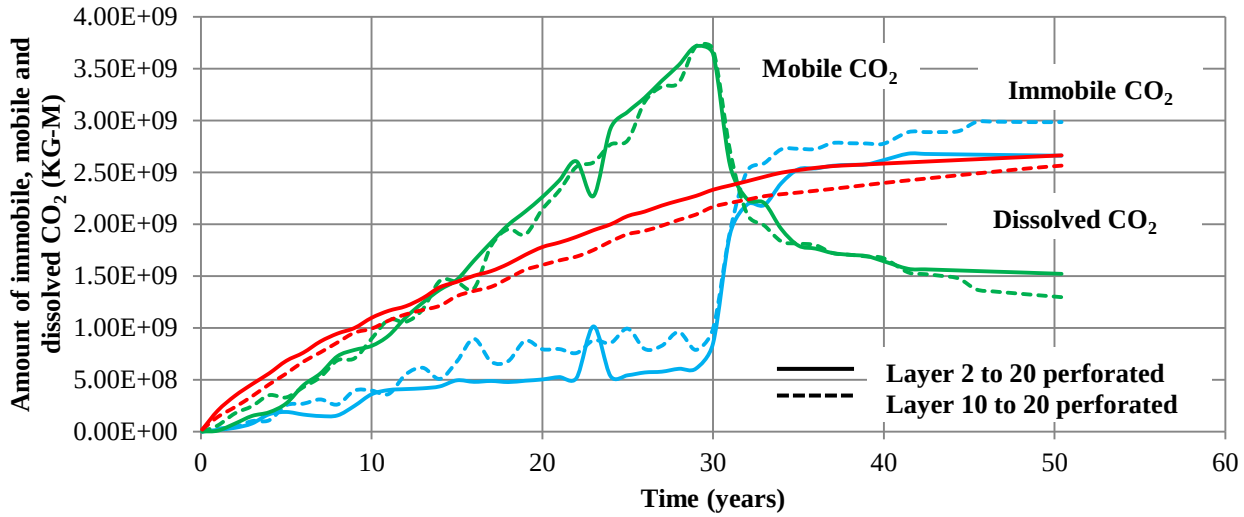

Figure 13 - Results of injected CO_2 in different phases from perforation interval variation.

Case No.	Perforation policy	Field pressure increase	Bottomhole pressure (bars)
1	Layer 2 to 20 perforated	10 %	109
2	Layer 10 to 20 perforated	9.6 %	126

Table 10 - Results of field pressure from perforation interval variation.

Horizontal Permeability

For an aquifer to be a potential candidate, permeability and porosity have to be high to provide sufficient storage volume for planned CO_2 storage. Seven different values of horizontal permeability are used: 50 mD, 100 mD, 200 mD, 250 mD, 300 mD, 400 mD and 500 mD for a constant Kv/Kh ration of 0.1.

High permeability enables CO_2 plume to migrate more laterally as seen in Figure 14. The gas plume beneath the seal layer is also formed earlier which results in bypassed lower layers which negatively affects sweep efficiency. On the other hand, for low permeability cases, CO_2 tends to accumulate around the wellbore and the areal extent of CO_2 plume is reduced due to the difficulty of migration. CO_2 is therefore stored in the lower layers which increases displacement efficiency. In terms of CO_2 phase distribution, for high permeability aquifers, CO_2 is stored more in gas phase and less dissolved in water or immobile phase, according to Figure 15 as gas rapidly moves through high permeability layers without being trapped by water. Results of pressure response are shown in Table 11, in terms of injectivity, higher bottomhole pressure is observed for low permeability aquifers as CO_2 migration path is disrupted and fluid pressure is increased. Therefore, low permeability gives poor injectivity. However, the effect on field pressure gives a converse result as higher permeability allows pressure to dissipate more quickly and laterally which leads to higher average field pressure increase.

In conclusion, horizontal permeability is one of the critical parameters which could positively or negatively impact CO_2 storage regarding different perspectives. Low permeability aquifers benefit pressure build-up, sweep efficiency and storage efficiency but worsen injectivity and vice versa.

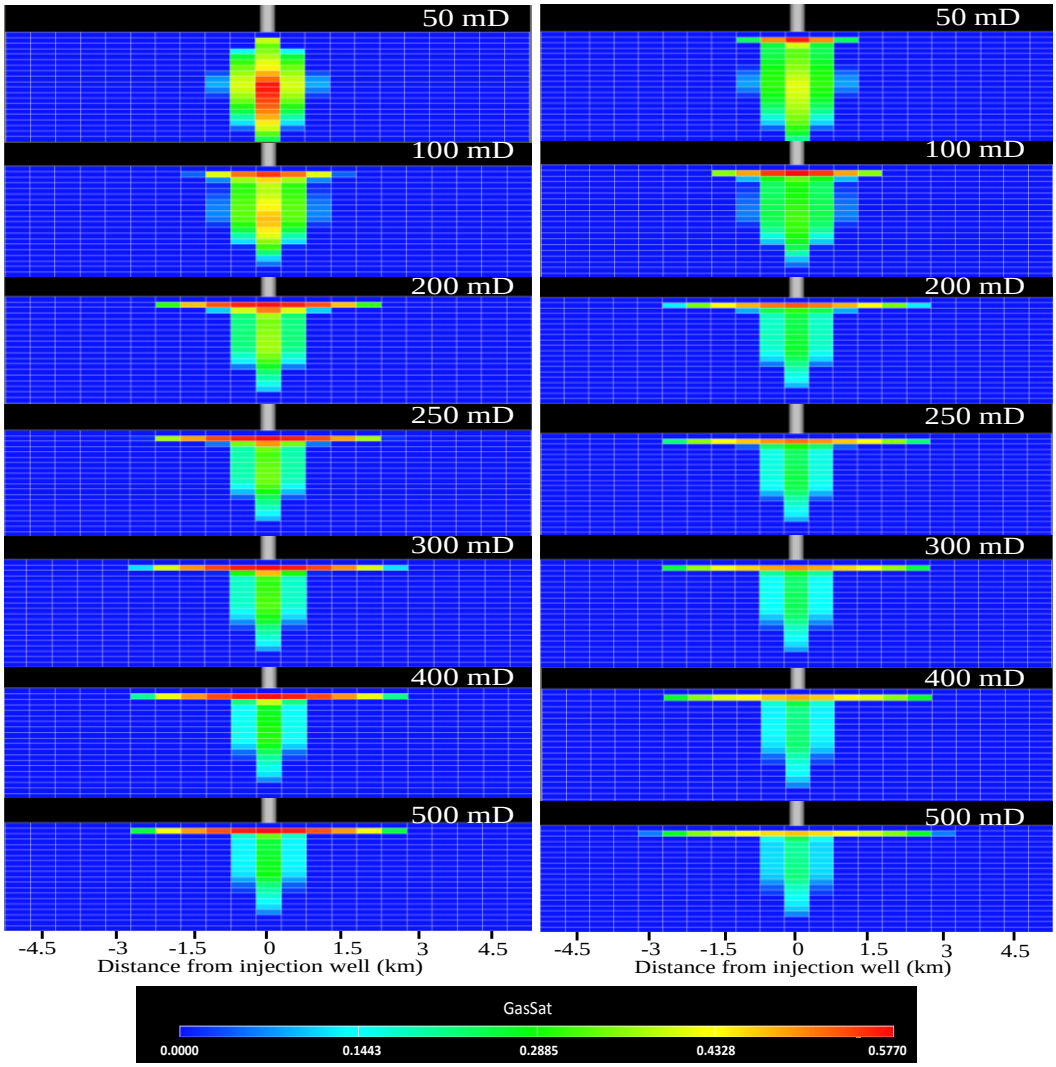

Figure 14 - CO_2 distribution at the injector from horizontal permeability variation *Left: at the end of the injection period (30 years) Right: at the end of the simulation period (50 years) Top to Bottom: Kh 50 mD, 100 mD, 200 mD, 250 mD, 300 mD, 400 mD, 500 mD.*

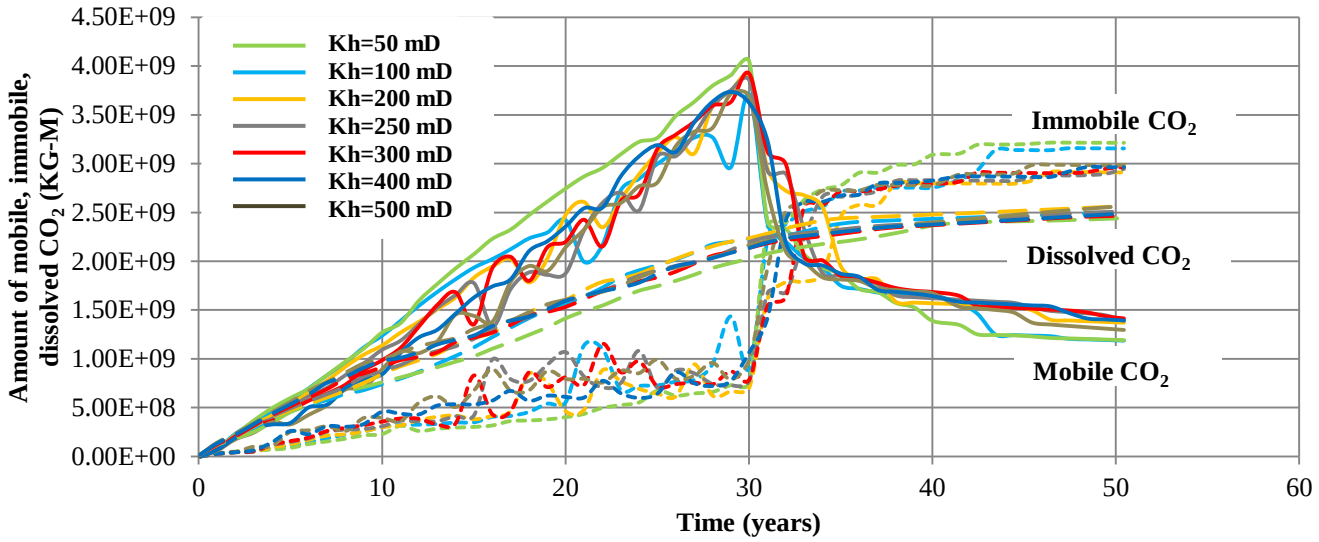

Figure 15 - Results of injected CO_2 in different phases from horizontal permeability variation.

Case No.	Kh	Field pressure increase	Average bottomhole pressure (Bars)
1	50 mD	6.7 %	140
2	100 mD	7.9 %	133
3	200 mD	8.9 %	130
4	250 mD	9.2 %	129
5	300 mD	9.4 %	128
6	400 mD	9.5 %	127
7	500 mD	9.6 %	126

Table 11 - Results of pressure increase and average bottomhole pressure from horizontal permeability variation.

Discussion

By observing CO_2 underground distribution at the injector, along with phase distribution over time, it can be concluded that gas initially accumulates around the wellbore and moves vertically until reaching the seal layer. The majority of CO_2 is stored in the form of mobile gas under the structural trap. Then, CO_2 plume is formed beneath the seal layer and gas tends to spread more horizontally. Highest gas saturation is always observed at the top of the aquifer layer at the injector. After the injection ceases, gas tends to spread more horizontally with higher gas saturation at the tail of the plume. Immobilization is dramatically enhanced at later times as water imbibes CO_2 and traps gas in the pore space. Dissolved gas is also present in relatively high amount due to the CO_2 solubility in brine with a gradual increase. In practical operations, storage security is the primary goal of CCS. The risk of CO_2 leakage can be alleviated by eliminating any escape paths which could possibly result from high seal permeability, comparatively small cap rock size and fracturing due to overpressure. However, cap rock thickness has no influence on CO_2 leakage as long as its permeability remains within the acceptable range.

Overall, three phases of gas are considered: mobile, immobile and dissolved. The most preferable trapping mechanism is in the form of an immobile phase since gas is securely stored in the pore space. While gas could find an escape path when stored in a mobile phase and the rate of dissolution relies on several conditions. Trapping mechanisms influence the storage security over time. Therefore, in earlier times of trapping process, cap rock integrity is very significant. Long term storage security can be enhanced by using high number of wells with only lower sections of the wells completed. Also, aquifer thickness and permeability play an important role: thicker aquifer and lower permeability give higher extent of immobilization. In practical operations, several perspectives have to be taken into account including commercial aspects. Storage optimization can be done by improving injectivity with fewer wells. Drilling more wells is therefore not commercially viable even though immobilization can be enhanced. One possibility is to use horizontal well in order to increase contacts between CO_2 and brine.

Areal sweep efficiency is small compared to vertical due to the effects of gravity segregation and viscous fingering. Displacement process is preferable when CO_2 is allowed to be stored in all of the layers and not aggregated around the wellbore or the top layers. Larger plume radius indicates that more gas easily migrates to the top part of the aquifer without being trapped which reduces the sweep efficiency. In order to obtain effective displacement, less injectors are to be used with only lower sections perforated. Also, aquifer thickness should be high, but with low permeability. The displacement process can be further optimized by injecting CO_2/brine mixture as mentioned in previous literature (Qi et al., 2009).

The main focus on this paper relies on the effect of several factors on pressure response. Considering practical operations, field pressure is normally maintained not to exceed the fracture pressure which results in the lack of CO_2 storage security. Pressure build-up occurs more extensively compared to the CO_2 plume. The effect of pressure can be observed beyond the radius of tens of kilometers while CO_2 disperses in the aquifer in the extent of 4-5 kilometers. This indicates the significance of pressure response on a laterally extensive aquifer area. The maximum field pressure is observed at the end of the injection period. Pressure build-up is expected to be relieved after a certain amount of time after the injection ceases, however, the pressure effect remains visible. In order to relieve pressure build-up, the aquifer should be enlarged in both area and thickness to allow higher extent of pressure dissipation in horizontal and vertical direction, respectively. Large aquifer volume is required in order to overcome the pressure limitation and thickness plays a more important role on pressure than area. Seal properties also impact pressure build-up: the thicker the seal, the lower the pressure build-up. However, the results are inconclusive for seal permeability since it could both positively and negatively impact the pressure response. Aquifer permeability has a negative influence on pressure build-up as high permeability allows pressure to dissipate more quickly resulting in higher average pressure build-up. In terms of completion policy, only lower sections of the wells should be perforated.

Pressure build-up greatly affects the maximum injection rate as if the pressure limitation were to be relaxed to 20% instead of 10%, the base case aquifer would be able to handle double the amount of injection. Also, a smaller aquifer would be required to safely store the target injection rate when the pressure limitation was relaxed. The proposed aquifer dimensions for this case (20% limit) would be the thickness of 882 m with the area of 3,850 km^2 or the thickness of 630 m with the area of 7,700 km^2, whereas the case with pressure limitation of 10%, the aquifer dimensions are the thickness of 1,260 m with the area of 3,850 km^2 or the thickness of 630 m with the area of 11,550 km^2. Moreover, if the pressure limit were to be 30%, the appropriate aquifer thickness would be half the size of the case with 10% limitation while the aquifer area would be one-third. This indicates that the aquifer dimensions are greatly sensitive to pressure response limitation. This limitation also relies on the integrity of the seal overlying the aquifer which should be properly defined by geomechanical tests.

Considering the well injectivity, higher injectivity results from lower bottomhole pressure which is preferable for operational perspective. This can be achieved by expansive aquifer area, high aquifer thickness and high horizontal permeability. In terms of well completion, more perforated area is preferable.

Summary and Conclusions

From the simulation studies, we conclude the following:

- Number of wells has no impact on pressure response as long as the total injection rate remains constant. However, larger number of wells enhances immobilization and dissolution, but lowers sweep efficiency.
- In terms of aquifer dimensions, thick aquifer benefits pressure build-up, immobilization, dissolution and injectivity. Lateral extensive aquifer lowers pressure effect and enhances injectivity without any impact on storage mechanisms. For the same aquifer volume, thickness plays a more important role on pressure response than area. By increasing the aquifer thickness, pressure impact can be more efficiently minimized compared to increasing the aquifer area. Therefore, the aquifer thickness is one of the most significant parameters on determining the injection feasibility.
- Cap rock should be continuous and extensive, at least covering the entire area of CO_2 plume in order to prevent CO_2 migration. Higher cap rock thickness could also lower pressure build-up. However, no effect of cap rock area or thickness on pressure response, injectivity, sweep efficiency and storage mechanisms are observed.
- CO_2 leakage is observed when seal permeability exceeds 0.5 mD. Seal permeability could affect pressure build-up both positively and negatively. Furthermore, seal permeability has no effect on bottomhole pressure or displacement efficiency.
- For well completion, only deeper layers of the aquifer should be perforated in order to minimize pressure build-up and enhance long-term storage security and sweep efficiency but this results in a reduced well injectivity.
- High value of horizontal permeability benefits higher injectivity but results in higher pressure build-up, poor sweep efficiency and greater amount of mobile gas.
- In order to store 10 Mtonnes/yr of CO_2 with the pressure limitation of 10%, the proposed aquifer dimensions are the area and thickness of at least 3,850 km^2, 1260 m or 11,550 km^2, 630 m, respectively. Appropriate cap rock area and thickness are 1,411 km^2 and 63 m, relatively with permeability of 0.1 mD or less.

Suggestion for Further Work

- A regional aquifer model is required in order to assess the real fracture pressure and large-scale pressure response.
- Previous studies already focused on the effect of injecting CO_2/brine in order to enhance sweep efficiency and hence increase storage capacity. However, this could cause excessive pressure according to the incompressibility of brine which needs further study.
- Heterogeneity should also be considered in the next step as Kv/Kh ratio tends to affect CO_2 migration path which results in pressure response.
- Well placement should also be studied as it may affect pressure distribution throughout the aquifer and vary the cap rock size.

Nomenclature

Kv	Vertical permeability
Kh	Horizontal permeability
Kr	Relative permeability
Krw	Water (brine) relative permeability
Krg	Gas relative permeability

References

Baklid, A., Korbol, R., & Owren, G. (1996, October 6-9). Sleipner Vest CO_2 Disposal,CO_2 Injection into a Shallow Underground Aquifer. *SPE 36600 SPE Annual Technical Conference and Exhibition* .

Bennion, D. B., & Bachu, S. (2006). Supercritical CO_2 and H_2S-Brine Drainage and Imbibition Relative Permeability Relationships for Intergranular Snadstone and Carbonate Formations. *SPE 99326* .

Bentham, M. (2006). *An Assessment of Carbon Sequestration Potential in the UK-Southern North Sea Case Study.* Tyndall Centre for Climate Change Research.

Bentham, M., & Kirby, G. (2005). CO_2 Storage in Saline Aquifers. *Oil & Gas Science and Technology - Rev. IFP , 60 (2005)* (No.3), 559-567.

Fenghour, A., Wakeham, W. A., & Vesovic, V. (1999). The Viscosity of Carbon Dioxide. *J. Phys. Chem. Ref. Data , 27*.

Flett, M., Gurton, R., & Taggart, I. (2004). The Function of Gas-Water Relative Permeability Hysteresis in the Sequestration of Carbon Dioxide in Saline Formations. *SPE 88485* .

Gale, J. (2004). Geological Storage of CO_2: What do we know, where are the gaps and what more needs to be done? *Energy 29 (2004) 1329-1338* .

Ghanbari, S., Al-Zaabi, Y., Pickup, G. E., Mackay, E., Gozalpour, F., & Todd, A. C. (2006). Simulation of CO_2 Storage in Saline Aquifers. *Chemical Engineering Research and Design* (84(A9)), 764-775.

Holloway, S., Vincent, C. J., & Kirk, K. L. (2006). *Industrial carbon dioxide emissions and carbon dioxide storage potential in the UK.*

Nottingham: British Geological Survey.

IPCC. (2005). *Special Report on Carbon dioxide Capture and Storage.* (B. Metz, Ed.)

Juanes, R., Spiteri, E. J., & Blunt, M. J. (2006). Impact of Relative Permeability Hysteresis on Geological CO_2 Storage. *Water Resour. Res. , 42*.

Kartikasurja, D. O., Lin, T. G., Sukahar, M. W., & Viratno, B. (2008). Study of Produced CO_2 Storage into Aquifer in an Offshore Field, Malaysia. *SPE 114553* .

Killough, J. E. (1976). Reservoir Simulation with History-dependent Saturation Functions. *Trans. AIME 261* , 37-48.

Kumar, A., Noh, M., Pope, G. A., Sepehmoori, K., Bryant, S., & Lake, L. W. (2004, April 17-21). Reservoir Simulation of CO_2 Storage in Deep Saline Aquifers. *SPE 89343 SPE/DOE Fourteenth Symposium on Improved Oil Recovery* .

Mo, S., & Akervoll, I. (2005, March 7-9). Modeling Long-term CO_2 Storage in Aquifer with a Black-oil Reservoir Simulator. *SPE 93951 SPE/EPA/DOE Exploration and Production Environmental Conference* .

Nghiem, L., Shrivastava, V., Kohse, B., Hassam, M., & Yang, C. (2009). Simulation of Trapping Processes for CO_2 Storage in Saline Aquifers. *Canadian International Petroleum Conference* .

Nicot, J.-P. (2008). Evaluation of large-scale CO_2 Storage on Fresh-water Sections of Aquifers: An Example from the Texas Gulf Coast Basin. *International Journal of Greenhouse Gas Control 2* , 582-593.

Oruganti, Y., & Bryant, S. L. (2009). Pressure Build-up During CO_2 Storage in Partially Confined Aquifers. *Energy Procedia 1* , 3315-3322.

Primera, A., Sifuentes, W., & Rodriguez, N. (2009, June 8-11). CO_2 Injection and Storage: A New Approach using Integrated Asset Modeling. *SPE 121970 SPE EUROPE/EAGE Annual Conference and Exhibition* .

Pruess, K., Xu, T., Apps, J., & Garcia, J. (2003, February 26-28). Numerical Modeling of Aquifer Disposal of CO_2. *SPE 83695 SPE/EPA/DOE Exploration & Production Environmental Conference* .

Qi, R., Beraldo, V., LaForce, T., & Blunt, M. J. (2009, November 11-14). Design of Carbon dioxide Storage in a North Sea Aquifer using Streamline-based Simulation. *SPE 109905 SPE Annual Technical Conference and Exhibition* .

Sifuentes, W., Blunt, M. J., & Giddins, M. A. (2009). Modeling CO_2 Storage in Aquifers: Assessing the Key Contributors to Uncertainty. *SPE 123582 2009 SPE Offshore Europe Oil & Gas Conference & Exhibition, 8-11 September 2009, Aberdeen, UK* .

Spycher, N., & Pruess, K. (2005). CO_2-H_2O mixtures in the Geological Seqeustration of CO_2 II Partitioning in Chloride Brines at 12-100 C and up to 600 bar. *Geochimica et Cosmochimica Acta , 69* (13), 3309-3320.

Suekane, T., Nobuso, T., Hirai, S., & Kiyota, M. (2008). Geological Storage of Carbon dioxide by Residual gas and Solubility trapping. *International Journal of Greenhouse Gas Control 2 (2008)* , 58-64.

van der Meer, L. (1992). Investigations regarding the Storage of Carbon dioxide in Aquifers in the Netherlands. *Energy Conversion & Management , 33 No. 5-8*.

van der Meer, L. (1992). Investigations Regarding the Storage of Carbon dioxide in the Netherlands. *Energy Conversion Management , 33* (No. 5-8), 611-618.

van der Meer, L., & van Wees, J. (2006, September 24-27). Limitations to Storage Pressure in Finite Saline Aquifers and the Effect of CO_2 Solubility on Storage Pressure. *SPE 103342 SPE Annual Technical Conference and Exhibition* .

Vandeweijer, V., Van der Meer, B., Kramers, L., Neele, F., Maurand, N., Gallo, Y. L., et al. (2009). CO_2 Storage in Saline Aquifer: In the Southern North Sea and Northern Germany. *Energy Procedia 1 (2009)* , 3079-3086.

Vesovic, V., Wakeham, W. A., Olchowy, G. A., Sengers, J. V., Watson, J., & Millat, J. (1990). The Transport Properties of Carbon Dioxide. *J. Phys. Chem. Ref. Data* , 19.

Yang, Q. (2008, October 20-22). Dynamic Modelling of CO_2 Injection in a Closed Saline Aquifer in the Browse Basin, Western Australia. *SPE 115236 SPE Asia Pacific Oil & Gas Conference and Exhibition* .

Zaytsev, I. D., & Aseyev, G. G. (1993). Properties of Aqueous Solutions of Electrolytes. *CRC Press* .

Zhou, Q., Birkholzer, J. T., Tsang, C.-F., & Rutqvist, J. (2008). A Method for Quick Assessment of CO_2 Storage Capacity in Closed and Semi-closed Saline Formations. *International Journal of Greenhouse Gas Control 2* , 626-639.

Thesis Appendix

Appendix A. Literature Review

A.1 Critical Literature Review Milestones

Paper number	Year	Title	Authors	Contribution
Energy Convers. Mgmt Vol.33, No.5-8, pp.611-618	1992	Investigations Regarding the Storage of Carbon dioxide in Aquifers in the Netherlands	L.G.H. van der Meer	First to mention injection limitation due to an increase in pore pressure
SPE 36600	1996	Sleipner Vest CO_2 Disposal, CO_2 Injection into a Shallow Underground Aquifer	Alan Baklid, Ragnhild Korbol and Geir Owren	
SPE 83695	2003	Numerical Modeling of Aquifer Disposal of CO_2	Karsten Pruess, Tianfu Xu, John Apps and Julio Garcia	Present capacity factors to evaluate the amount of CO_2 that can be trapped into various phases
SPE 89343	2004	Reservoir Simulation of CO_2 Storage in Deep Saline Aquifers	A. Kumar, M. Noh, G.A. Pope, K. Sepehrnoori, S. Bryant and L.W. Lake	Define the significance of each trapping mechanism. Also, study the impact of reservoir parameters on storage efficiency.
Energy 29 (2004) 1361-1369	2004	Demonstrating Storage of CO_2 in Geological Reservoirs: The Sleipner and SACS Project	Tore A. Torp and John Gale	First project to store CO_2 in an aquifer, also numerical simulation proves the feasibility of the idea
SPE 93951	2005	Modeling Long-Term CO_2 Storage in Aquifer with a Black-Oil Reservoir Simulator	S. Mo and I. Akervoll	Present results of long-term CO_2 storage by using a black-oil simulator
SPE 103342	2006	Limitations to Storage Pressure in Finite Saline Aquifers and the Effect of CO_2 Solubility on Storage Pressure	L.G.H. van der Meer and J.D. van Wees	First to address the effect of solubility on storage pressure
SPE 109905	2007	Design of Carbon dioxide Storage in a North Sea Aquifer Using Streamline-Based Simulation	Ran Qi, Valcir Beraldo, Tara LaForce and Martin J. Blunt	First to present injection scheme of injecting CO_2 and brine followed by brine to optimize capillary trapping
SPE 114553	2008	Study of Produced CO_2 Storage into Aquifer in an Offshore Field, Malaysia	Dewanto Odeara Kartikasurja, Helix RDS, Tan giok Lin, M. Wakif Sukahar, Bernato Viratno	An example of investigating the feasibility of CO_2 storage of an actual aquifer by simulation studies and economic analysis
SPE 115236	2008	Dynamic Modelling of CO_2 Injection in a Closed Saline Aqufier in the Browse Basin, Western Australia	Qingjun Yang	Address pressure buildup problem as injection carries on while address an injection-drainage strategy to relieve the problem.
International Journal of Greenhouse Gas Control 2 (2008) 582-593	2008	Evaluation of Large-scale CO_2 Storage on Fresh-water Sections of Aquifers: An Example from the Texas Gulf Coast Basin	Jean-Philippe Nicot	First attemp to study the effect of up-dip displacement of brine on fresh-water resources and evaluate the time scale for pressure relaxation
International Journal of Greenhouse Gas Control 3 (2009)	2008	Large-scale Impact of CO_2 Storage in Deep Saline Aquifers: A Sensitivity Study on Pressure Response in	Jens T. Birkholzer, Quanlin Zhou, and Chin-Fu Tsang	Investigate the region of influence from CO_2 injection in terms of brine displacement and pressure preturbation

181-194		Stratified System		
SPE 121970	2009	CO_2 Injection and Storage : A New Approach Using Integrated Asset Modeling	A. Primera, W. Sifuentes, and N. Rodriguez	Study the feasibility by the use of an integrated approach, coupling surface facilities with fluid flow model
SPE 123582	2009	Modeling CO_2 Storage in Aquifers : Assessing the Key Contributors to Uncertainty	W. Sifuentes, M. J. Blunt, and M.A. Giddins	Uncertainties study of physical properties focusing on the impact on dissolution and residual gas trapping
SPE 125848	2009	Simulation of CO_2 Storage in Saline Aquifers	Long Nghiem, Vijay Shrivastava, David Tran, Bruce Kohse, Mohamed Hassam, and Chaodong Yang	Study the physics of residual gas and solubility trapping mechanisms and identify the optimization strategy. Also, mention geomechanics simulator to predict caprock potential.
Energy Procedia 1 (2009) 3079-3086	2009	CO_2 Storage in Saline Aquifers: In the Southern North Sea and Northern Germany	Vincent Vandeweijer, Bert van der Meer, Leslie Kramers, Filip Neele, Nicolas Maurand, Yann Le Gallo, Dan Bossie-Codreanu, Frauke Schafer, David Evans, Karen Kirk, Christian Bernstone, Sarah Stiff and Wilson Hull	Simulation study of aquifers in the North Sea and in Germany by the use of SIMED II (TNO) and COORES (IFP)
Energy Procedia 1 (2009) 3315-3322	2009	Pressure Build-up During CO_2 Storage in Partially Confined Aquifers	YagnaDeepika Oruganti, Steven L. Bryant	Study the effect of aquifer compartmentalization and rock compressibility regarding aquifer pressure response

A.2 Critical Literature Review

Energy Conversion Management Vol.33 No.5-8, pp.611-618, 1992
Investigations Regarding the Storage of Carbon dioxide in Aquifers in the Netherlands

Authors: L.G.H. van der Meer

Contribution to the understanding of CO_2 storage in aquifers
This paper compiles different ideas and concerns of CO_2 storage. Also, injection limitation according to pressure effect is first mentioned.

Objective of the paper
This paper presents the technical feasibility, limitations and consequences of carbon dioxide storage in aquifers. The issues considered are physical processes while CO_2 is stored, the geochemical and environmental aspects and the underground CO_2 storage capacity is evaluated.

Methodology used
Two hypothetical CO_2 storage reservoirs are considered in order to estimate their potential for long-term storage of CO_2. Several aspects of information is integrated and summarized.

Conclusion reached
1. In terms of feasibility, the CO_2 storage technology is feasible.
2. Displacement processe is dominated by gravity segregation and viscous fingering which affects the areal and vertical sweep efficiency.
3. The constraints for a feasible storage aquifer are aquifer depth, permeability, seal and structural trap existence.
4. CO_2 injection scheme is considered to be safe as any risks can be mitigated by prior planning and intensive control.
5. The aquifer storage capacity of the Nether lands is estimated to be 1.2 Gton.

Comments
The author discussed the feasibility and limitations in broad perspectives and not in details. Actual experiments or simulation studies should have been performed.

SPE 36600
Sleipner Vest CO_2 Disposal, CO_2 Injection into a Shallow Underground Aquifer

Authors: Alan Baklid and Ragnhild Korbol, and Geir Owren

Contribution to the understanding of CO_2 storage in aquifers
Sleipner project is the first project to inject CO_2 into an offshore underground aquifer. Since the aquifer is shallow, several problems are mentioned.

Objective of the paper
1. To discuss the CO_2 disposal technique of injecting into an aquifer by performing simulation studies
2. To discuss the injection facilities and the well and reservoir aspects in order to design the injection strategy

Methodology used
CO_2 to be disposed came from the Sleipner project gas production. First, several disposal alternatives were discussed. The option of injecting CO_2 into an underground aquifer was selected and the target was the Utsira Formation. A simulation study of 20 years injection period was carried out to investigate how CO_2 would migrate in the formation. Injection scheme and well design were studied based on the amount of disposed CO_2 of 1.7 MSm^3 per day.

Conclusion reached
CO_2 was to be disposed into a shallow underground aquifer. One well was drilled with an appropriate distance from other wells. Also, to allow for safe and cost effective handling of the CO_2, an injection system was designed to give a constant back pressure from the well corresponding to the output pressure from the compressor and be independent of the injection rate. It was accomplished by selecting high injectivity sand, completing the well with a large bore, and regulating the dense phase CO_2 temperature.

Comments

SPE 83695
Numerical Modeling of Aquifer Disposal of CO_2

Authors: Karsten Pruess, Tianfu Xu, John Apps and Julio Garcia

Contribution to the understanding of CO_2 storage in aquifers
This paper mentioned the affected radius from pressure perturbation.

Objective of the paper
This paper studies the amounts of CO_2 to be trapped into various phases for a range of conditions that may be encountered in typical aquifers. Also, the storage capacity of saline aquifers is estimated in terms of storage capacity factors by using volumetric averages, the frontal displacement theory and numerical simulation.

Methodology used
Realistic PVT properties for brine and CO_2 were used in the simulation studies.
Capacity factors for gas-, liquid-, and solid-phase storage were defined by using volumetric estimates and numerical simulation. A realistic fluid property description of brine/CO_2 mixtures for supercritical conditions was taken into account.

Conclusion reached
The amount of precipitated CO_2 may be comparable to the amount of dissolved CO_2 in preferable conditions. For typical conditions of the aquifer, CO_2 is stored in different phases in the order of 30 kg/m2 of aquifer volume.

Comments
The paper gives particular interest on geochemical modeling.

SPE 89343
Reservoir Simulation of CO_2 Storage in Deep Saline Aquifers

Authors: A. Kumar, M. Noh, G.A. Pope, K. Sepehrnoori, S. Bryant and L.W. Lake, The University of Texas at Austin

Contribution to the understanding of CO_2 storage in aquifers
This paper clarifies the significance of storage mechanisms as well as studies the impact of several parameters.

Objective of the paper
1. To study the significance of each storage mechanism by the use of simulation studies
2. To study the impact of several parameters on the storage efficiency, including average permeability, the ratio of vertical to horizontal permeability, residual gas saturation, salinity, temperature, aquifer dip angle, permeability heterogeneity and mineralization

Methodology used
A natural gradient flow simulation was run for 1000 to 100000 years in order to define the storage mechanisms. Pure supercritical CO_2 is injected into the aquifer for ten years. The injector then shut in. This study assumed an open aquifer with constant pressure boundaries and no conductive faults to avoid the potential escape route for mobile CO_2. Average aquifer properties were used in the base case model to represent a generic aquifer. Several simulation sets are conducted to study the impact of the parameters. In terms of fluid properties, experimental data sets were used to define solubility and brine density. Maximum bottomhole pressure was controlled.

Conclusion reached
1. The effect of residual gas on CO_2 storage can be very large.
2. Aquifer dip and horizontal to vertical permeability ratio have a significant effect on gas migration.
3. Well completions play an important role as if the supercritical CO_2 enters near the top seal, it is likely to continue to migrate up dip and may find an escape path, while if CO_2 is injected in the bottom half of the aquifer, gravity-driven flow steadily reduces the amount of mobile gas before it can migrate to the top of the aquifer.
4. Mineralization plays a significant role if only the rate of gravity-driven gas movement is sufficiently small.
5. The amount of CO_2 stored as an immobile phase can be larger than the CO_2 stored in brine and minerals.

Comments
The aquifer properties used in the model are not referred to, therefore the properties may not represent the actual aquifer properties.

Energy 29 (2004) 1361-1369
Demonstrating Storage of CO_2 in Geological Reservoirs: The Sleipner and SACS Project

Authors: Tore A. Torp and John Gale

Contribution to the understanding of CO_2 storage in aquifers
The Sleipner project is currently an ongoing project which proves the potential of the storage method. By monitoring the movement of CO_2 after the injection, the theory proposed can be verified.

Objective of the paper
To elaborate the significance and method of SACS/SACS2 project, as well as, discuss the long-term effect of CO_2 storage in geological reservoirs.

Methodology used
SACS/SACS2 project aims to monitor CO_2 behavior underground by incorporating seismic survey and geochemical and reservoir simuation.

Conclusion reached
The Sleipner project proves that CO_2 storage in aquifers is safe and has a low environment impact. The geochemical and reservoir simulation shows that CO_2 can be safely stored in the aquifer for thousands of years.

Comments
The Utsira formation is a large and porous aquifer which proves to have great efficiency in storing CO_2. However, other aquifers may not have the same properties, therefore, more issues are to be discussed before implementing any further projects.

SPE 93951
Modeling Long-Term CO_2 Storage in Aquifer with a Black-Oil Reservoir Simulator

Authors: S. Mo and I. Akervoll

Contribution to the understanding of CO_2 storage in aquifers
This paper gives an alternative of analyzing the impact of various reservoir parameters by using a black-oil simulator instead of a compositional simulator.

Objective of the paper
To present the result of modeling long-term CO_2 storage in a shallow saline aquifer by focusing on the sensitivity of CO_2 distribution in the deposit with respect to critical CO_2 saturations during the injection period and to residual CO_2 saturation for water reentering CO_2 filled volumes. Also, to study the impact of various reservoir parameters, including average permeability, vertical to horizontal permeability ratio relative permeability and capillary pressure.

Methodology used
Realistic CO_2/water phase behavior covering all pressure, temperature and compositional conditions accounted for during the simulations was used. Simulation studies were performed using a black-oil simulator.

Conclusion reached
1. A black-oil simulator with an explicit setting of PVT data for CO_2/brine mixtures can be used in CO_2 injection modeling.
2. If the reservoir has an effective vertical communication, the dissolution of CO_2 in brine is the dominant mechanism of CO_2 storage.
3. The amount of trapped CO_2 gas decreases when kv/kh increases.

Comments

SPE 103342
Limitations to Storage Pressure in Finite Saline Aquifers and the Effect of CO_2 Solubility on Storage Pressure

Authors: L.G.H. van der Meer and J.D. van Wees

Contribution to the understanding of CO_2 storage in aquifers
This paper emphasizes the effect of injection additional fluid in to an aquifer on fluid volumes and pressures relating to CO_2 solubility. The author mentioned the Sleipner project which is normally refered to in order to prove the feasibility of CO_2 injection into saline aquifers. However, the Sleipner Utsira storage formation is an extensive and thick aquifer and only about 1 Mtonnes of CO_2 is injected annually. Pressure can be distributed over a large area for this case, but for other aquifers which may not have comparatively similar size or properties, pressure limitation can occur.

Objective of the paper
1. To study various aspects of the solution processes based on numerical simulation
2. To find out the pressure effects of CO_2 solubility on the total storage capacity

Methodology used
First, a Norwegian type of open aquifer storage location was studied to explore various aspects of the solution process. Then, the Mid-European type of aquifer was used in order to study the impact of CO_2 solubility on storage pressure.

Conclusion reached
1. Solubility offers a storage potential in the long term (>1000 years) due to the accumulation of CO_2 in the gas phase, which has a limited contact with the water phase.
2. The amount of CO_2 in the free gas phase can be reduced by contacting CO_2 to as much fresh water as possible or by extending migration path laterally.
3. Equilibrium solubility accounts for about 10-20% mass percent of CO_2 being dissolved.
4. Moving or migrating CO_2 will dissolve much faster than stationary CO_2.
5. CO_2 solubility will have a pressure-reducing effect.
6. In order to optimize well placement, it is recommended to increase the inter-well spacing to distribute the pressure more evenly.

Comments
Dissolved CO_2 cannot be disregarded in terms of pressure. After injection ceases, CO_2 is converted from one phase to another which has a pressure-reducing effect, but will never go down to zero.

SPE 109905
Design of Carbon Dioxide Storage in a North Sea Aquifer Using Streamline-Based Simulation

Authors: Ran Qi, Valcir Beraldo, Tara LaForce and M.J. Blunt

Contribution to the understanding of CO_2 storage in aquifers
This paper proposes a new injection strategy of injection CO_2 and brine followed by brine alone which is cost-effective and could enhance capillary trapping.

Objective of the paper
To design injection scheme for optimal storage efficiency, as well as, minimizing the amount of water injected by focusing on capillary trapping

Methodology used
Pore-scale modeling, as well as field-scale streamline-based simulator, was performed. One-dimensional results were verified through comparison with analytical solutions. Also, three-dimensional simulation was performed with the use of the SPE10 model representing a heterogeneous sandstone North Sea aquifer.

Conclusion reached
By injecting CO_2 with a fractional flow between 85 to 100% followed by a short period of chase brine, CO_2 would become immobile in pore-scale droplets. This enhances storage efficiency by trapping CO_2 in the porous rock without having to rely on caprock integrity. Also, this injection scheme is cost-effective.

Comments
In practical aquifer storage operations, the majority of CO_2 is initially stored as a mobile phase. Residual trapping becomes more significant at later times when injection ceases. Therefore, optimizing residual trapping can only enhance storage capacity in a limited extent.

SPE 114553
Study of Produced CO_2 Storage into Aquifer in an Offshore Field, Malaysia

Authors: Dewanto Odeara Kartikasurja, Tan giok Lin, M. Wakif Sukahar, Bernato Viratno

Contribution to the understanding of CO_2 storage in aquifers
This paper studies the feasibility of the storage in an actual field together with the economic studies which give the idea of actual potential of the CO_2 sequestration method.

Objective of the paper
This paper aims at studying a part of a field development plan for the B field in Malaysia by focusing on the management and disposal of CO_2 from the ongoing production. Geological formation was evaluated and simulation studies were performed. A number of parameters were considered in optimizing the storage capacity without disturbing an overlying gas reservoir.

Methodology used
The disposal site was first selected by concerning seal integrity, reservoir quality and storage capacity. A black oil simulator was used and some parameters were tuned in order to account mutual solubilities between CO_2 and H_2O. Peng-Robinson EOS was used to calculate CO_2 properties. Sensitivity on number of wells and aquifer volume was run in order to meet the gas injection rate target.

Conclusion reached
1. The aquifer proposed is feasible in order to store CO_2 as it has sufficient capacity, also the formation water has low salinity which enables CO_2 to dissolve more readily and reduces excessive pressure build-up.
2. High injectivity wells are significant in order to minimize the bottomhole pressure required in order to stay below fracture pressure. The wells should be drilled with maximum deviation to enhance the injectivity.
3. The number of wells required depends on the size of the aquifer, the target injection rate and well injectivity.
4. By lengthening the CO_2 migration path, dissolution process is enhanced and pressure build-up is minimized.
5. Low salinity brine is preferable in order to maximize the amount of CO_2 dissolved.

Comments
This paper uses a different method of modeling dissolved gas in water phase which is by an indirect modeling method in black oil simulator. Also, it mentions the significance of well injectivity.

SPE 115236
Dynamic Modelling of CO_2 Injection in a Closed Saline Aqufier in the Browse Basin, Western Australia

Authors: Qingjun Yang

Contribution to the understanding of CO_2 storage in aquifers
This paper mentions the problem of pressure buildup as the injection carries on. Also, an injection-drainage strategy was introduced in order to mitigate the problem which enables closed saline aquifers to store CO_2 effectively.

Objective of the paper
To study dynamic modeling of CO_2 Injection in the Browse Basin, Western Australia and optimize the injection strategy

Methodology used
First, analytical models were run to study the pressure buildup, then numerical simulation using Eclipse 100 was performed to investigate how this closed system can be made appropriate for CO_2 storage. Also, an injection scheme was optimized.

Conclusion reached
From numerical simulation results, the injection pressure increased rapidly which is mainly caused by the inability of the reservoir to accommodate displaced water. Therefore, a drainage strategy was used to relieve the injection pressure. Also, certain factors were regarded to optimize the drainage scheme, including storage efficiency, the risk of CO_2 breakthrough, and the cost of draining brine. In order to prevent CO_2 breakthrough to the drainage well in high permeability model, bottomhole pressure of free-flowing well is to be maintained. In terms of well design, horizontal wells are preferable and only lower layers should be perforated to prevent CO_2 migration.

Comments
This is a very useful paper as it mentions the problem of pressure buildup and introduces a solution. However, the risk of CO_2 breakthrough due to gravity segregation and viscous fingering is fairly high and needs to be addressed on further.

International Journal of Greenhouse Gas Control 2 (2008) 582-593
Evaluation of Large-scale CO_2 Storage on Fresh-water Sections of Aquifers: An Example from the Texas Gulf Coast Basin

Authors: Jean-Philippe Nicot

Contribution to the understanding of CO_2 storage in aquifers
This paper is the first attempt to study the effect of up-dip displacement of brine on fresh-water resources.

Objective of the paper
This paper studies the conditions needed for shallow groundwater to be impacted by up-dip displacement of brines. Also, the time scale for pressure relaxation is investigated.

Methodology used
A relatively well-know aquifer in the Texas Gulf Coast is chosen as the aquifer model. CO_2 is injected at the rate per well of 1 or 5 Mt/year in 50 years over 50 years. CO_2 is injected in the down-dip layers. Large-scale impact is observed in terms of pressure and brine leakage.

Conclusion reached
In the Gulf Coast Basin, water displacement will likely not be a major concern to the fresh water up-dip sections of formations into which CO_2 is injected. After 50 years of injection, an average water-table rise is approximately 1 m, with minor increase in stream baseflow and larger increase in groundwater evapotranspiration, but no significant change in salinity.

Comments

International Journal of Greenhouse Gas Control, 3, 2009
Large-scale Impact of CO_2 Storage in Deep Saline Aquifers: A Sensitivity Study on Pressure Response in Stratified Systems

Authors: Jens T. Birkholzer, Quanlin Zhou, and Chin-Fu Tsang

Contribution to the understanding of CO_2 storage in aquifers
This paper investigates the region of influence from CO_2 injection in terms of brine displacement and pressure preturbation. Also, sensitivity analysis on pore compressibility and seal permeability were performed.

Objective of the paper
1. To develop a basic understanding of flow and pressure conditions in a CO_2 storage formation embedded in a sequence of aquifers and aquitards
2. To explore the effects of interlayer communication through low-permeability seals and the impact on lateral/vertical displacement
3. To determine the vertical and lateral region of influence during/after injection of CO_2 and evaluating possible implications for shallow groundwater resources

Methodology used
Numerical simulation was performed on an open multilayer ground water system to determine the region of influence in both lateral and vertical directions. The model includes eight aquifers and eight aquitards with large lateral extent in order to ensure the minimal effect of boundary condition on the simulation results. The period of simulation run is 100 years; 30 years of injection period and 70 years of post-injection period. TOUGH2/ECON simulator is used. Injection rate is controlled at 1.52 Mtonnes/year. Sensitivity on pore compressibility, seal permeability

Conclusion reached
1. Considerable pressure build-up in the storage formation is predicted more than 100 km away from the injection zone, while the lateral brine transport velocity and migration distance are less significant.
2. Seal permeability has a great impact on pressure buildup and brine displacement behavior. Seals with high permeability allow for considerable brine leakage which results in the reduced pressure buildup compared to the perfect seal of low or close-to-zero permeability.

Comments

SPE 121970
CO_2 Injection and Storage: A New Approach Using Integrated Asset Modeling

Authors: A. Primera, W. Sifuentes, and N. Rodriguez

Contribution to the understanding of CO_2 storage in aquifers
This paper gives the idea of integrated analysis which could prevent the misleading estimation of the storage capacity by standalone simulation. Also, CO2STORE option was activated.

Objective of the paper
This paper proposed an integrated approach study to couple reservoir models with surface facilities to model fluid flow behavior of the asset. Also, different injection variables were studied including facilities, well completion and number of wells.

Methodology used
An integrated asset model, comprising the reservoir, the network and the integrated control model, was used. The model was built with representative information from the North Sea with the use of three injectors. Simulation was run using Eclipse with fixed bottomhole pressure control. Also, CO2STORE option was activated to employ the solubility model. A network model was introduced in order to evaluate the effect of surface facilities. Sensitivity analysis was also performed in order to investigate the impact of certain reservoir properties, e.g. porosity, horizontal permeability, salt concentration, residual gas saturation and vertical permeability, on the storage efficiency.

Conclusion reached
In order to attain the accurate capacity of CO_2 storage, network analysis should be performed.

Comments
The idea of integrated analysis is very feasible as it gives more accurate storage efficiency which should be performed for further implementation.

SPE 123582
Modeling CO_2 Storage in Aquifers: Assessing the Key Contributors to Uncertainty

Authors: W. Sifuentes, SPE, Schlumberger; M. J. Blunt, SPE, Imperial College; M.A. Giddins, SPE, Schlumberger

Contribution to the understanding of CO_2 storage in aquifers
This paper evaluates the influence of different parameters on the efficiency of trapping mechanism. This analysis will help determine the optimum case for CO_2 storage in aquifers.

Objective of the paper
This paper studies the influence of different physical properties on the effectiveness of CO_2 storage in aquifers by focusing on the impact on dissolution and residual trapping.

Methodology used
Simulation studies were performed by the use of a compositional simulator incorporating CO2STORE option. A specific geological model of an aquifer in Ketzin, Germany was built. The model was initially saturated with brine; CO_2 was then injected over 40 years. Only one injection well was used. Sensitivity analysis was run to obtain a qualitative picture and understanding of the variation of different parameters, including reservoir parameters (temperature, salinity, permeability, residual gas saturation, dip and pressure), model parameters (cell block size), operational parameters and others (injection strategies, well locations, well completions and hysteresis effects).

Conclusion reached
1. Horizontal permeability is the most influential parameter on the amount of CO_2 dissolved.
2. Residual gas saturation is the most influential parameter on the amount of residual CO_2.
3. Hysteresis has to be considered in the case of residual trapping.
4. Operational parameters, such as well placement, well completion and injection schemes are considered significant. Wells completed at the deeper depth lead to higher amount of CO_2 trapped. WAG technique also enhances the storage.

Comments
A variety of parameters were studied in terms of the impact on only dissolution and residual trapping. The impact on the overall trapping mechanisms should also be studied.

SPE 125848

Simulation of CO_2 Storage in Saline Aquifers

Authors: Long Nghiem, SPE, Vijay Shrivastava, SPE, David Tran, SPE, Bruce Kohse, SPE, Mohamed Hassam, SPE, Chaodong Yang, SPE, Computer Modelling Group Ltd.

Contribution to the understanding of CO_2 storage in aquifers

This paper explains in details about the physical processes occurring during CO_2 storage relating with the use in simulations. Also, geomechanics simulator is mentioned as it is able to model failure of caprock.

Objective of the paper

1. To describe the features of physical processes that occur during the storage of CO_2
2. To study the optimization of residual gas and solubility trapping
2. To study geomechanics simulator to model the failure of caprock which leads to the leakage of CO_2

Methodology used

Greenhouse simulator, GEM, was used to run the model in order to describe the important physics involved. Several equation sets representing various types of trapping mechanisms were input. Also, a geomechanic modeling was performed to observe cap rock deformation resulting from excess injection rate.

Conclusion reached

1. Solubility trapping and residual gas trapping are competitive.
2. Residual gas trapping is important in low-permeability aquifers and water injection can help accelerate the storage.
3. Mineral trapping is a very slow process.
4. It is feasible to predict the potential failure of the caprock by the use of geomechanics simulator.

Comments

Only the optimization of two types of trapping, residual gas and solubility trapping, were studied. However, mineral trapping is proved to be the safest storage mechanism which should also be studied.

Energy Procedia 1 (2009) 3079-3086
CO_2 Storage in Saline Aquifers: In the Southern North Sea and Northern Germany

Authors: Vincent Vandeweijer, Bert van der Meer, Leslie Kramers, Filip Neele, Nicolas Maurand, Yann Le Gallo, Dan Bossie-Codreanu, Frauke Schafer, David Evans, Karen Kirk, Christian Bernstone, Sarah Stiff and Wilson Hull

Contribution to the understanding of CO_2 storage in aquifers
This paper gives the properties of a North Sea aquifer.

Objective of the paper
1. To optimize the injection rate
2. To study the migration behavior of CO_2
3. To design injection well locations

Methodology used
Two geological models were created; one in the Southern North Sea and one in Northern Germany, in order to investigate the results in two different aquifer structures. For the Southern North Sea model, the properties and geology of the aquifer were known. However, for the German aquifer, there was no information on facies or petrophysical parameters and three scenarios were generated; homogeneous, varied porosity and permeability. The simulation was carried out with SIMED II (TNO) and COORES (IFP).

Conclusion reached
The injection rate was optimized and the well was placed in the high permeability area.

Comments

Energy Procedia 1 (2009) 3315-3322
Pressure build-up during CO_2 storage in partially confined aquifers

Authors: YagnaDeepika Oruganti, Steven L. Bryant

Contribution to the understanding of CO_2 storage in aquifers
This paper studies the effect of faults, number of faults and rock compressibility on aquifer pressure by considering the variation in viscosity of the fluids with depth.

Objective of the paper
1. To discuss the risk factors involved in fracturing the seal or activating a fault caused by pressure build-up
2. To evaluate injectivity limitations with the existence of sealing faults
3. To assess the number of wells and well placement
4. To study the effect of aquifer depth on pressure build-up

Methodology used
Compositional simulations (GEM) are used with different locations and geometries of sealing faults in aquifers, with several values of rock compressibility. The injection rate is equivalent to the emission rate from coal-fired power plants. CO_2 injectivity vs. time and pressure profile in the aquifer were the parameters evaluated in order to obtain the risk factors caused by pressure issue.

Conclusion reached
1. Sealing faults do not affect injectivity as long as it is beyond the radial extent of the CO_2 plume. Greater number of sealing faults which are close to the injector causes elevated pressures to propagate farther.
2. Rock compressibility has little influence on pressure profile.
3. Depth of the aquifer has a significant effect on pressure build-up. Lower injectivity and higher pressure build-up are observed in shallower aquifers due to the high sensitivity of brine viscosity to pressure and temperature.
4. Pressure build-up extends much farther than the CO_2 plume.

Comments

Appendix B. CO_2 Emission and Global Climate Change

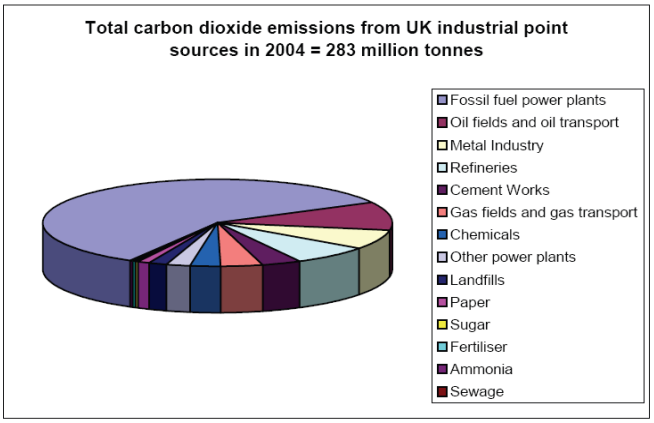

Figure B.1 - Breakdown of CO_2 emissions from industrial point sources in the UK (Data from the Environment Agency, SEPA and Northern Ireland DoE,2004, Diagram from Holloway, 2006).

No.	Facility Name	CO_2 emissions (Mt, rounded)
1	Drax Power Station	20.5
2	West Burton Power Station	9.2
3	Ratcliffe on Soar Power Station	9.2
4	Cottam Power Station	9.0
5	Longannet Power Station	8.8
6	Ferrybridge ‘C’ Power Station	8.0
7	Kingsnorth Power Station	7.8
8	Eggborough Power Station	7.3
9	Scunthorpe Steel Works	7.2
10	Port Talbot Steel Works	6.6

Table B.1 - CO_2 emissions from the 10 largest industrial point sources (Holloway, 2006).

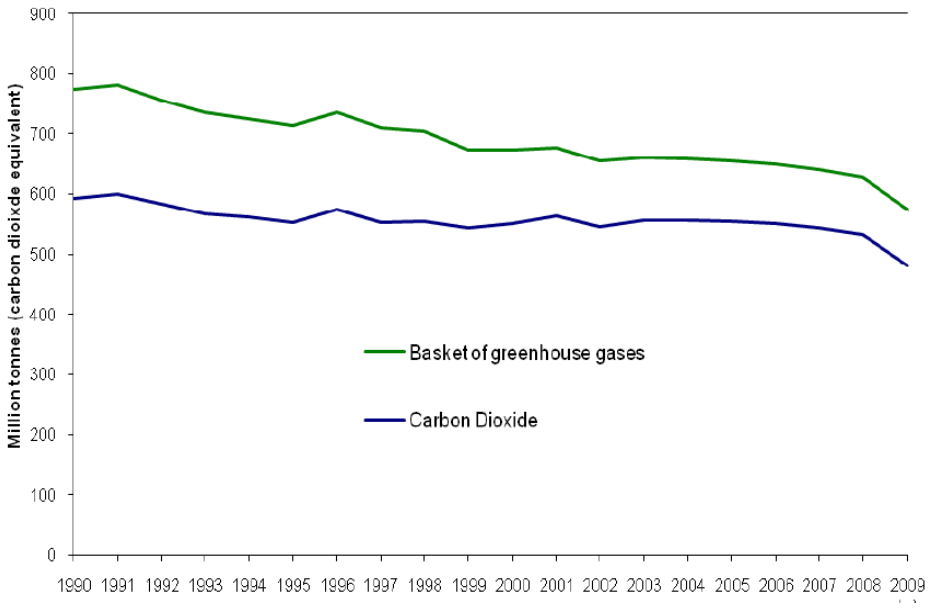

Figure B.2 - Emissions of greenhouse gases, 1990-2009 (provisional) (DECC, 2010).

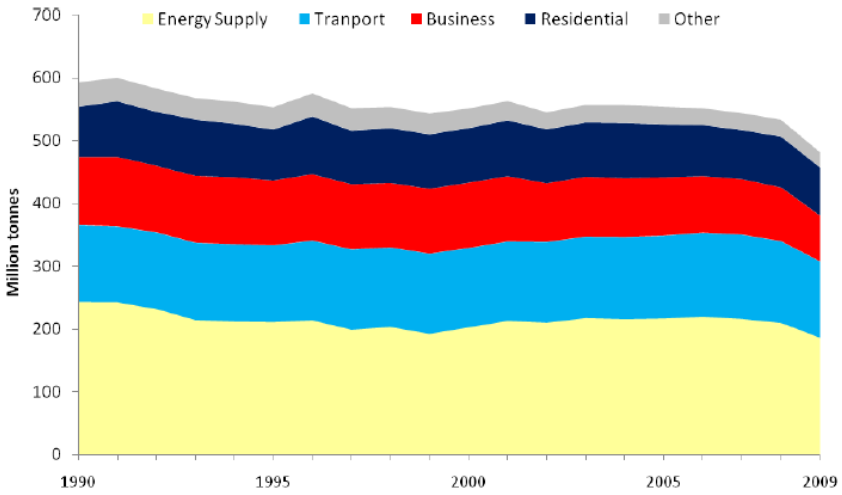

Figure B.3 - Carbon dioxide emissions by source, 1990-2009 (provisional) (DECC, 2010).

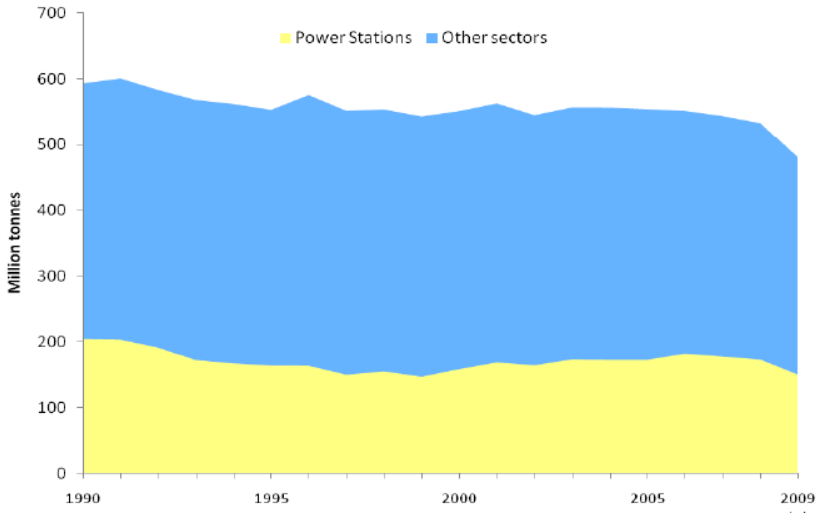

Figure B.4 - Carbon dioxide emissions from electricity generated at power stations, 1990-2009 (provisional) (DECC, 2010).

Appendix C. Model Initialization

Appendix C.1 Solubility Modeling

Spycher et al. (2003) first proposed the calculation of mutual solubility of CO_2 and H_2O by using Redlich-Kwong equation of state to express the deviation from ideal behavior. Aqueous solubility constants for gaseous and liquid $CO_2$are generated in the range of temperature from 15 to 100 °c and for H_2O and from 12 to 110 °c for CO_2 and up to 600 bars. Then, Spycher & Pruess (2005) presented the methods of mutual solubility calculation to account for the effect of chloride salts by including activity coefficients for aqueous CO_2.

The form of Redlich-Kwong equation is as follows (Redlich & Kwong, 1949):

$$P = \left(\frac{RT}{V-b}\right) - \left(\frac{a}{T^{0.5}V(V+b)}\right) \quad (1)$$

where a: a constant representing represents measures of intermolecular attraction
b: a constant representing measures of intermolecular repulsion
V: volume of compressed gas phase
P: pressure
T: temperature
R: gas constant

The values of k_o, k_1 and b are fitted from P-V-T data.

$$a = k_0 + k_1 T \quad (2)$$

For binary mixture, a_{mix} and b_{mix} replace a and b.

$$a_{mix} = \sum_{i=1}^{n}\sum_{j=1}^{n} y_i y_j a_{ij} \quad (3)$$

$$b_{mix} = \sum_{i=1}^{n} y_i b_i \quad (4)$$

The calculation of mutual solubilities which accounts for the effect of salts is as follows:

$$y_{H_2O} = \frac{K^0_{H_2O} a_{H_2O}}{\emptyset_{H_2O} P_{tot}} exp\left(\frac{(P-P^0\bar{V}_{H_2O})}{RT}\right) \quad (5)$$

$$x_{CO_2} = \frac{\emptyset_{CO_2}(1-y_{H_2O})P_{tot}}{55.508\gamma'_x K^0_{CO_2(g)}} exp\left(-\frac{P-P^0\bar{V}_{CO_2}}{RT}\right) \quad (6)$$

$$y_{H_2O} = \frac{1-B-x_{salt}}{\left(\frac{1}{A}\right)-B} \quad (7)$$

$$x_{CO_2} = B(1-y_{H_2O}) \quad (8)$$

The equations are preferably expressed in the form of molality instead of mole fraction.

$$x_{salt} = \frac{\vartheta m_{salt}}{55.508 + \vartheta m_{salt} + m_{CO_{2(aq)}}} \quad (9)$$

$$y_{H_2O} = \frac{(1-B)55.508}{\left(\frac{1}{A}-B\right)(\vartheta m_{salt}+55.508)+\vartheta m_{salt}B} \quad (10)$$

where x_{salt}: the mole fraction of the dissolved salt
m: molality
ϑ: stoichiometric number of ions contained in the dissolved salt
y_{H_2O}: water mole fraction in the CO_2-rich phase
x_{CO_2}: CO_2 mole fraction in the aqueous phase
K^0: thermodynamic equilibrium constant at temperature T and reference pressure P^0 = 1 bar
$\bar{V}$: average partial molar volume of each pure condensed phase
ø: fugacity coefficient of each component in the CO_2-rich phase
γ'_x: activity coefficient for aqueous CO_2

Appendix C.2 Relative Permeability and Capillary Pressure Data

Relative permeability data is taken from experimental data of supercritical CO_2-brine at in-situ conditions of the Viking Formation sandstone, Alberta, Canada (Bennion & Bachu, 2006). Capillary pressure is calculated by using Van Genuchten method (1980).

$$P_c = P_o((S^*)^{-1/\lambda} - 1)^{1-\lambda} \quad (11)$$

$$S^* = \frac{S_w - S_{wr}}{1-S_{wr}} \quad (12)$$

Assuming λ = 0.7 and P_0 = 10 kPa
P_0: entry capillary pressure
λ : exponential value
S_{wr}: irreducible water saturation
P_c: capillary pressure
S_w: water saturation

Drainage				Imbibition	
Sw	**Krg**	**Krw**	**Pc (bars)**	**Sw**	**Krg**
0.423	0.264	0.000		0.423	0.264
0.452	0.228	0.006	35.875	0.437	0.215
0.481	0.195	0.019	26.462	0.451	0.174
0.510	0.166	0.038	22.034	0.465	0.139
0.538	0.140	0.062	19.342	0.479	0.109
0.567	0.116	0.091	17.340	0.493	0.085
0.596	0.096	0.125	15.795	0.507	0.065
0.625	0.078	0.163	14.536	0.521	0.048
0.654	0.062	0.205	13.468	0.535	0.035
0.683	0.048	0.251	12.534	0.549	0.025
0.711	0.037	0.301	11.722	0.563	0.018
0.740	0.028	0.355	10.949	0.577	0.012
0.769	0.020	0.413	10.223	0.591	0.008
0.798	0.014	0.474	9.527	0.605	0.005
0.821	0.009	0.539	8.985	0.619	0.003
0.856	0.006	0.608	8.157	0.633	0.002
0.885	0.003	0.679	7.443	0.647	0.001
0.913	0.002	0.755	6.699	0.661	0.001
0.942	0.001	0.833	5.807	0.675	0.000
0.971	0.000	0.915	4.624	0.689	0.000
1.000	0.000	1.000	0.000	0.703	0.000

Table C.1 - Relative permeability data (Bennion & Bachu, 2006).

For the seal layer, capillary pressure is calculated by the use of the Leverett J-function in order to account for the impact of permeability on capillary pressure.

$$J(S_w) = P_c\sqrt{\frac{K}{\emptyset}}\frac{1}{\gamma cos\theta} \quad (13)$$

where Sw: water saturation
Pc: capillary pressure
K: permeability
$\emptyset$: porosity
γ: surface tension
θ: contact angle

Appendix C.3 Hysteresis

Figure C.1 represents a typical relative permeability curves for a non-wetting phase. The process starts with water saturating the entire aquifer then, when gas is injected, drainage process occurs following the path from 1 to 2. Water saturation decreases as gas saturation increases. Then, at the tail of the plume, imbibition process occurs as water saturation increases to point 3. However, if the drainage process is reversed at point 4, the saturation path will follow the scanning curve and end at point 5.

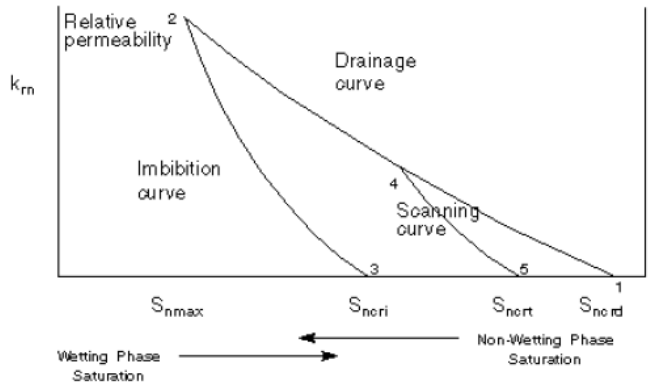

Figure C.1 - A typical pair of relative permeability curves for a non-wetting phase (Eclipse technical manual 2009, Schlumberger, 2009).

There are several methods of generating the scanning curves: Carlson's method, J. Jargon's method and Killough's method. Killough's method is used in this paper.

The following equations are used in the calculation.

$$S_{ncrt} = S_{ncrd} + \frac{S_{hy} - S_{ncrd}}{1 + C(S_{hy} - S_{ncrd})} \quad (14)$$

$$C = \frac{1}{S_{ncri} - S_{ncrd}} - \frac{1}{S_{n\,max} - S_{ncrd}} \quad (15)$$

The relative permeability for a particular saturation S_n on the scanning curve is

$$K_{rn}(S_n) = \frac{K_{rni}(S_{norm}) K_{rnd}(S_{hy})}{K_{rnd}(S_{n\,max})} \quad (16)$$

$$S_{norm} = S_{ncri} + \frac{(S_n - S_{ncrt})(S_{n\,max} - S_{ncri})}{S_{hy} - S_{ncrt}} \quad (17)$$

S_{hy}: maximum non-wetting phase saturation reached in the run
K_{rni}: relative permeability value on the bounding imbibitions curve
K_{rnd}: relative permeability value on the bounding drainage curve
$S_{n\,max}$: maximum saturation of the gas phase
S_{ncri}: critical saturation of the imbibitions curve
S_{ncrt}: critical saturation of the scanning curve

Appendix C.4 CO_2 Density and Viscosity

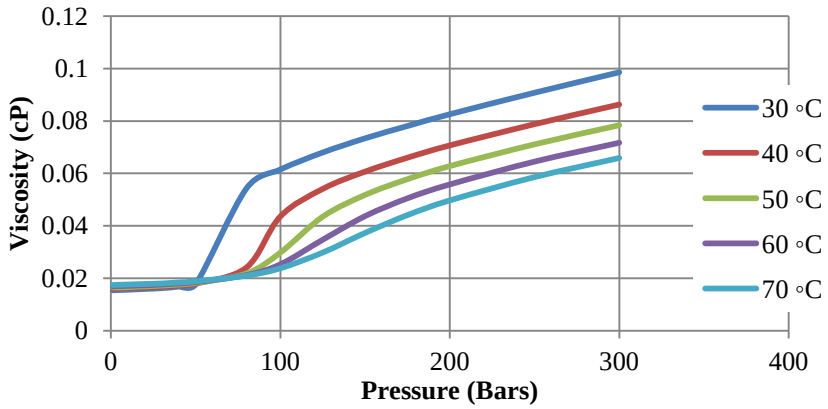

Figure C.2 - CO_2 viscosity for different temperatures (calculated based on Vesovic et al., 1990 and Fenghour et al., 1999).

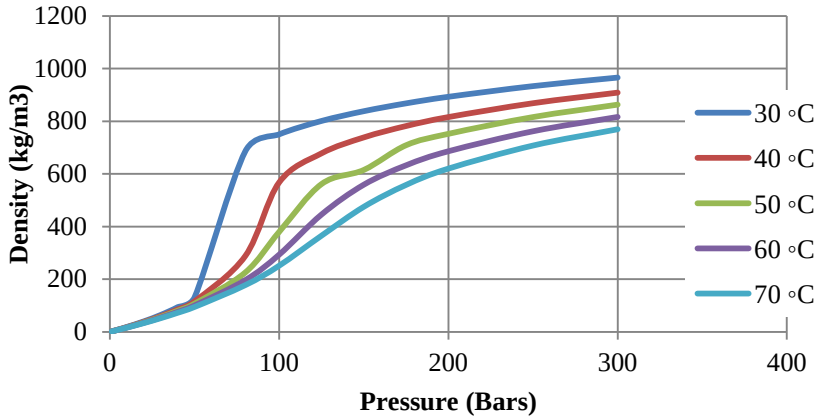

Figure C.3 - CO_2 density for different temperatures (calculated based on Peng Robinson equation of state).

Appendix D. Results

Appendix D.1 Injection Rate and Number of Wells

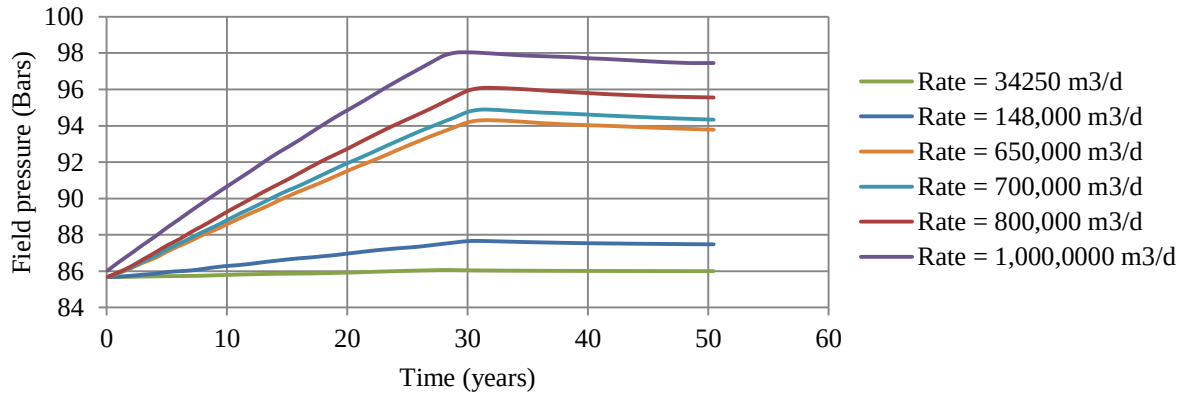

Figure D.1 - Field pressure from injection rate variation.

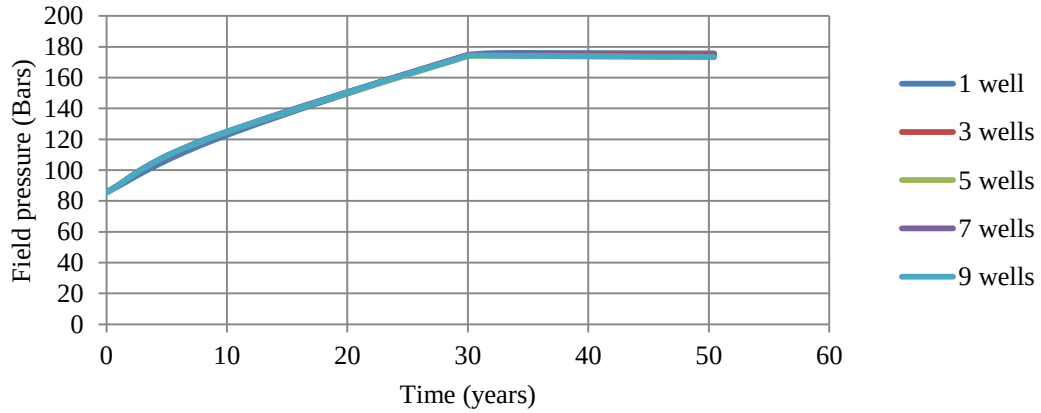

Figure D.2 - Field pressure from number of wells variation.

Appendix D.2 Aquifer Dimensions

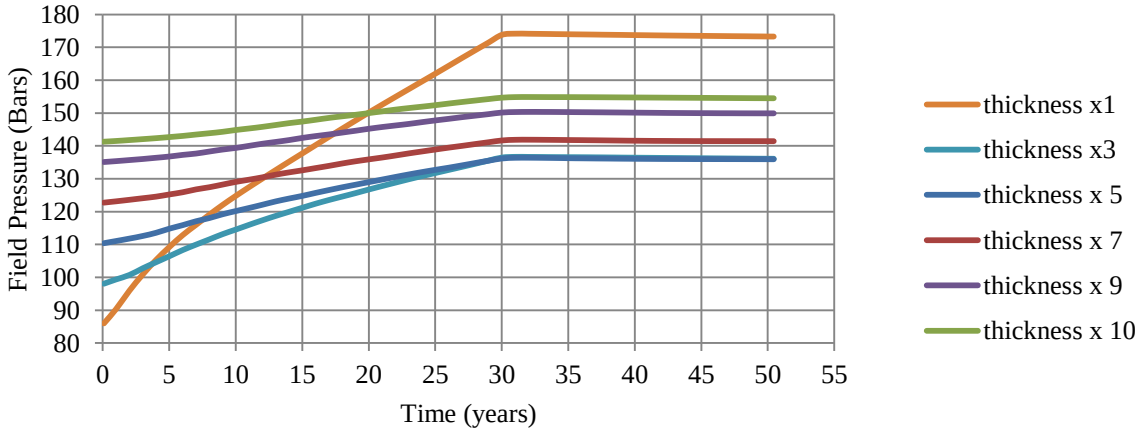

Figure D.3 - Field pressure from aquifer thickness variation.

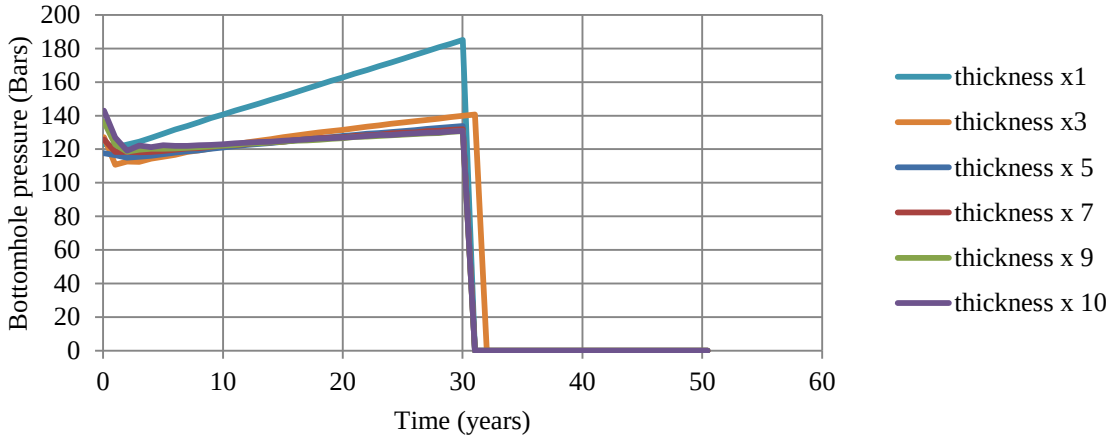

Figure D.4 - Bottomhole pressure from aquifer thickness variation.

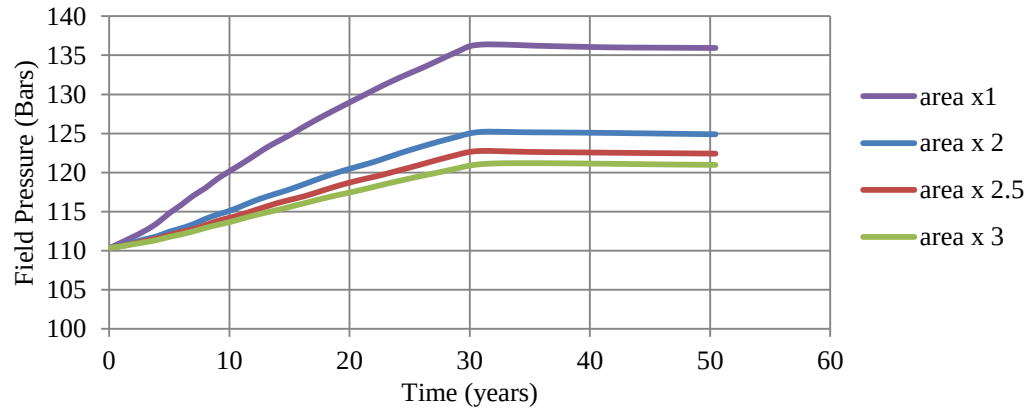

Figure D.5 - Field pressure from aquifer area variation.

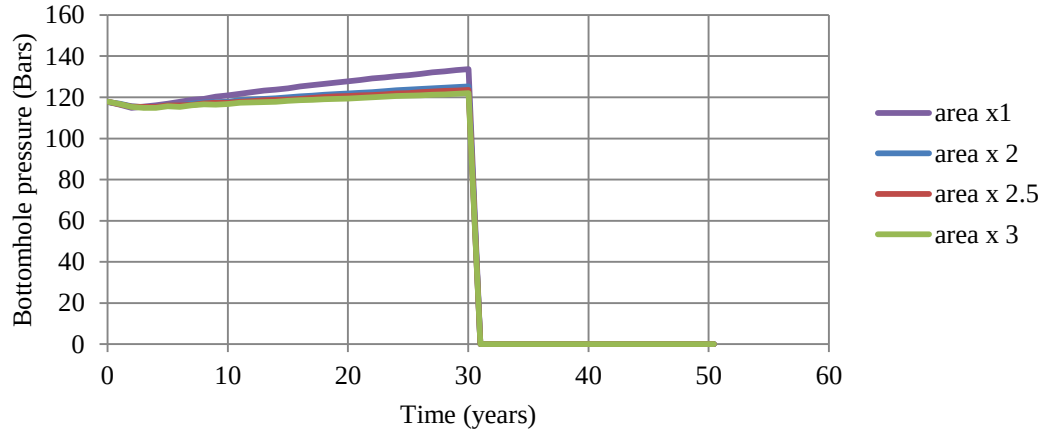

Figure D.6 - Bottomhole pressure from aquifer area variation.

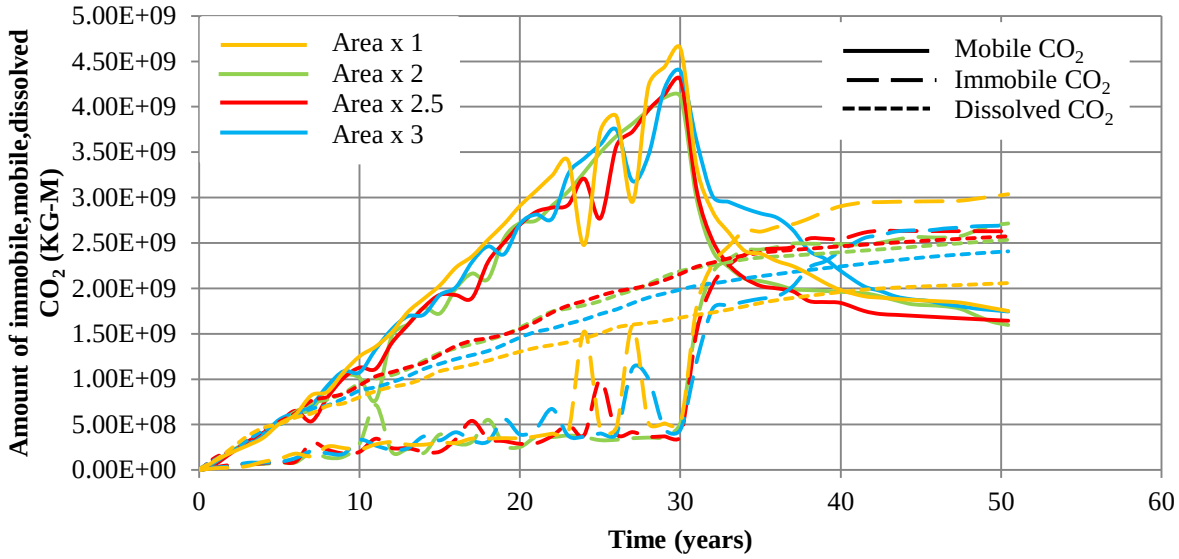

Figure D.7 - CO_2 phase distribution from aquifer area variation.

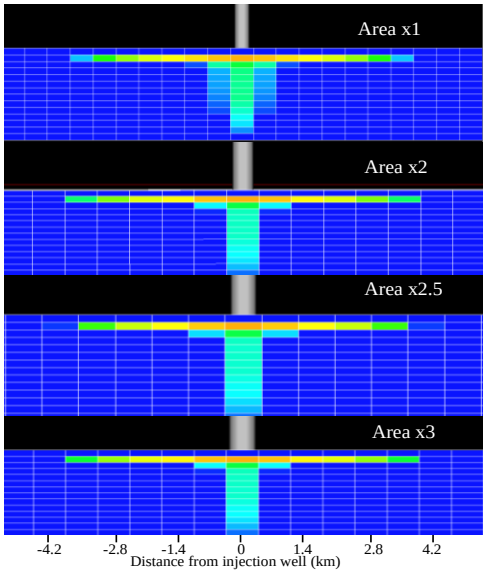

Figure D.8 - CO_2 distribution at the injector at the end of the simulation period (50 years) from aquifer area variation.

Appendix D.3 Cap rock size

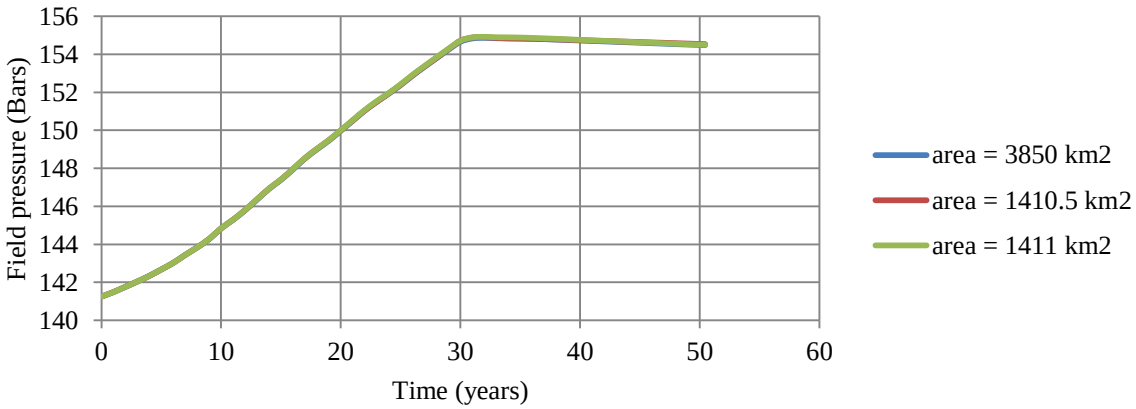

Figure D.9 - Field pressure from cap rock area variation.

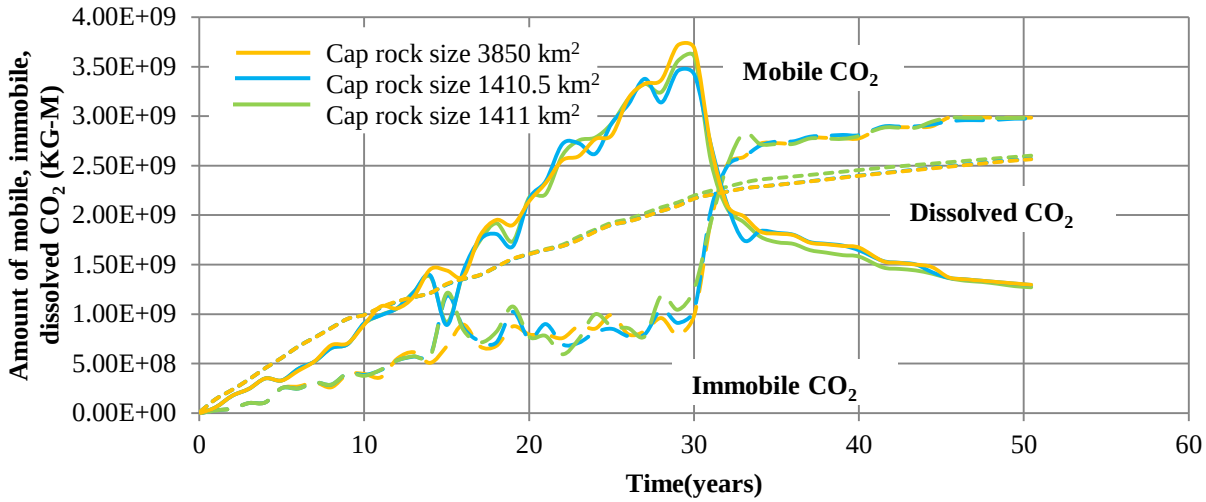

Figure D.10 - CO_2 phase distribution from cap rock area variation.

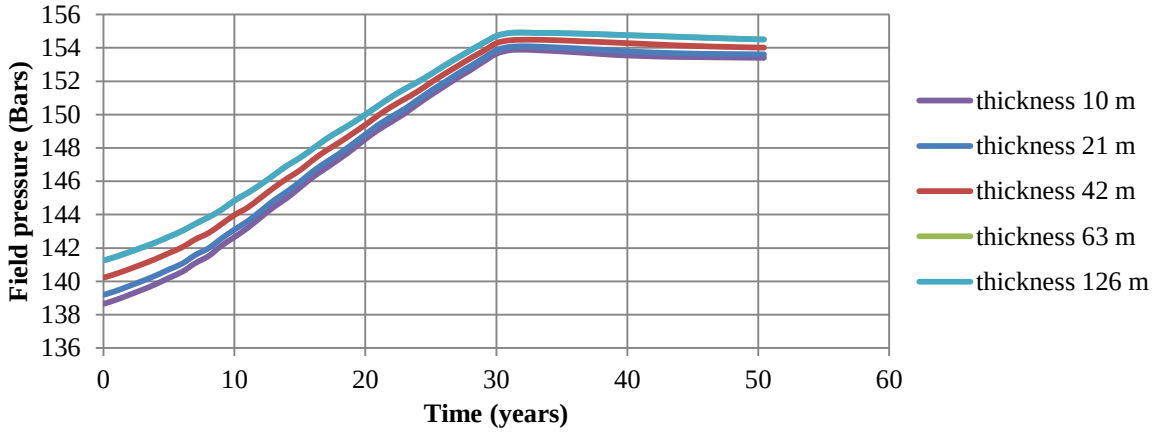

Figure D.11 - Field pressure from cap rock thickness variation.

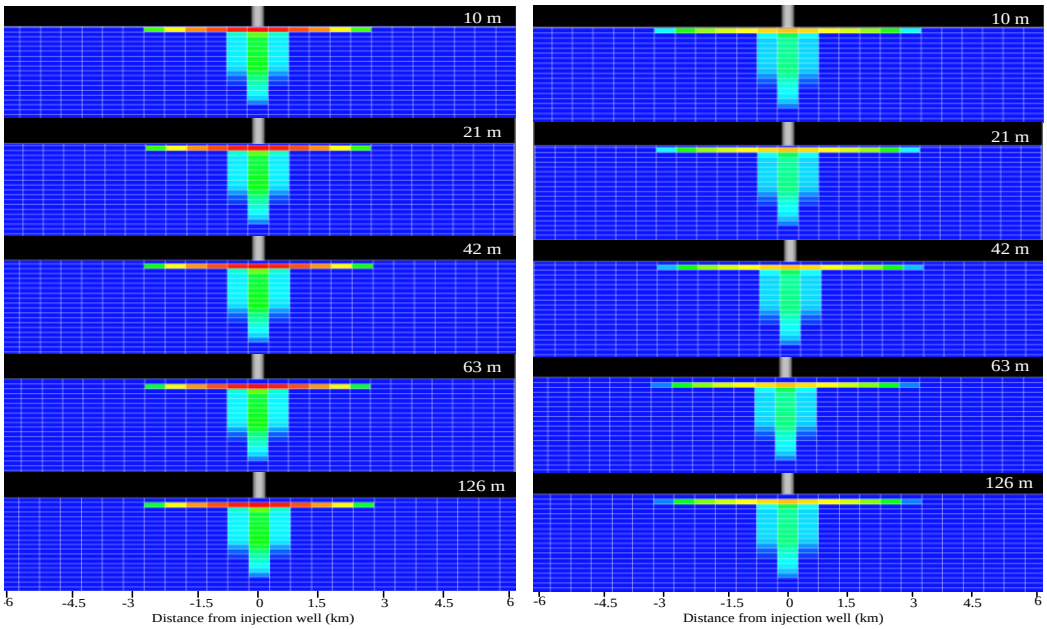

Figure D.12 - 2D side view of CO_2 distribution at the injector from cap rock thickness variation *Top to bottom: Cap rock thickness 10 m, 21m, 42 m, 63 m Left: at the end of the injection period (30 years) Right: at the end of the simulation period (50 years).*

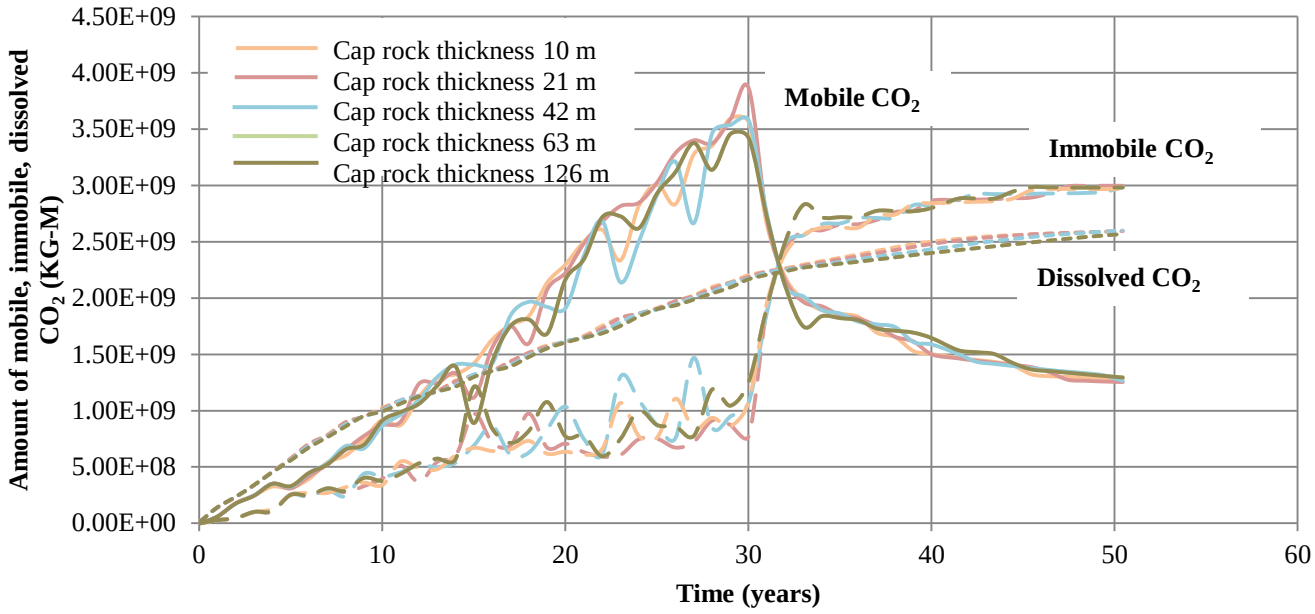

Figure D.13 - CO_2 phase distribution from cap rock thickness variation.

Appendix D.4 Seal Permeability

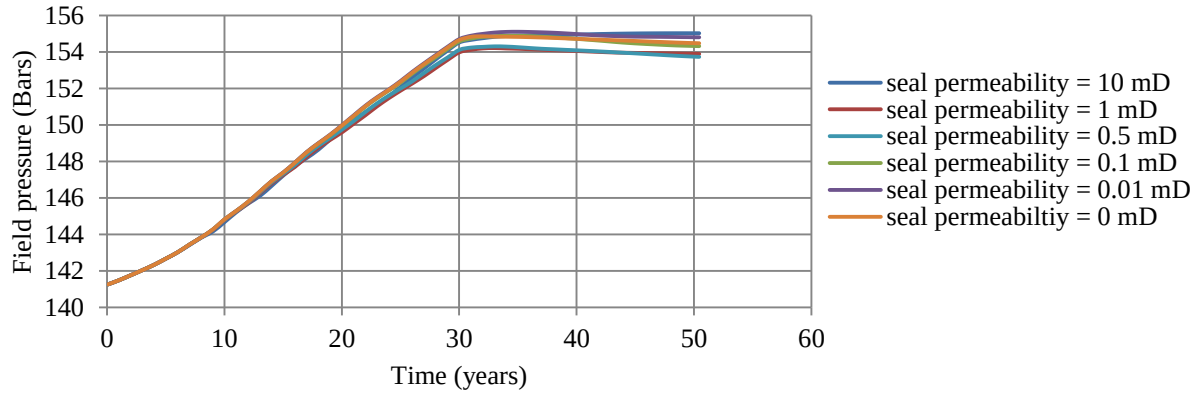

Figure D.14 - Field pressure from seal permeability variation.

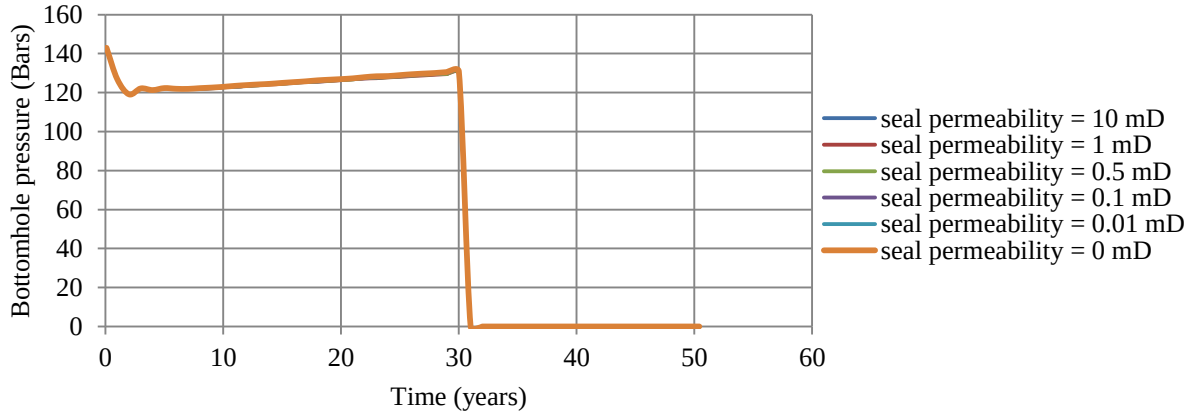

Figure D.15 - Bottomhole pressure from seal permeability variation.

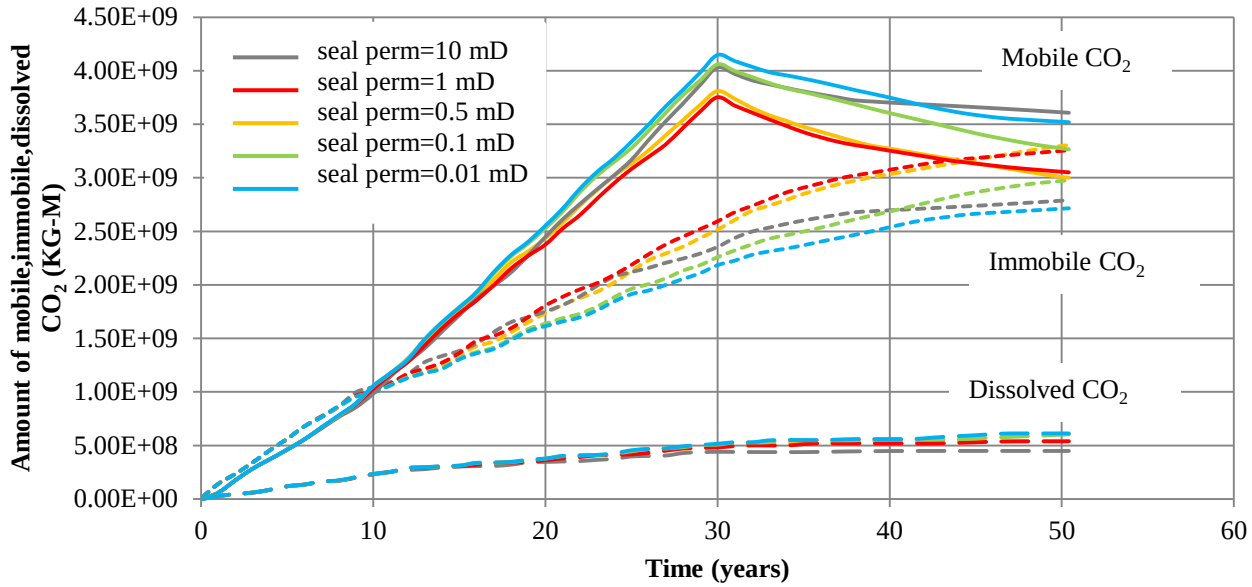

Figure D.16 - CO_2 phase distribution from seal permeability variation.

Appendix D.5 Perforation interval

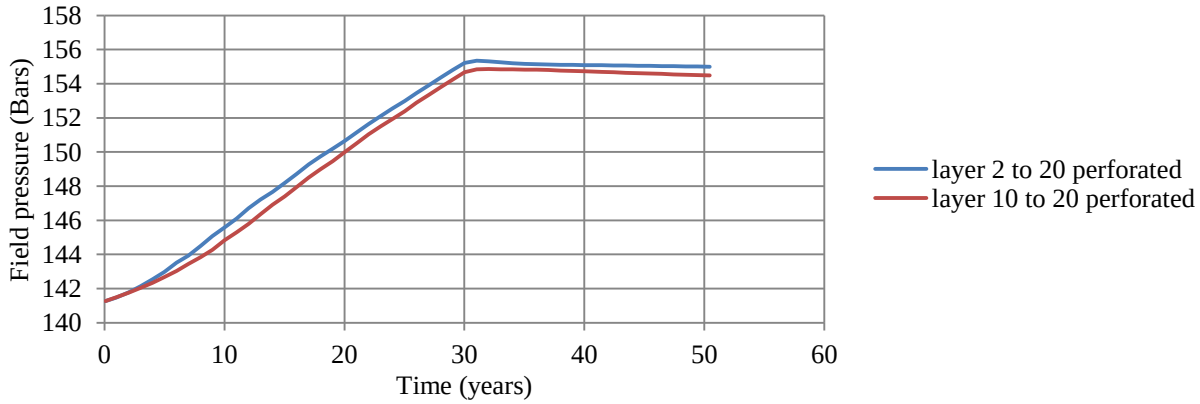

Figure D.17 - Field pressure from perforation interval variation.

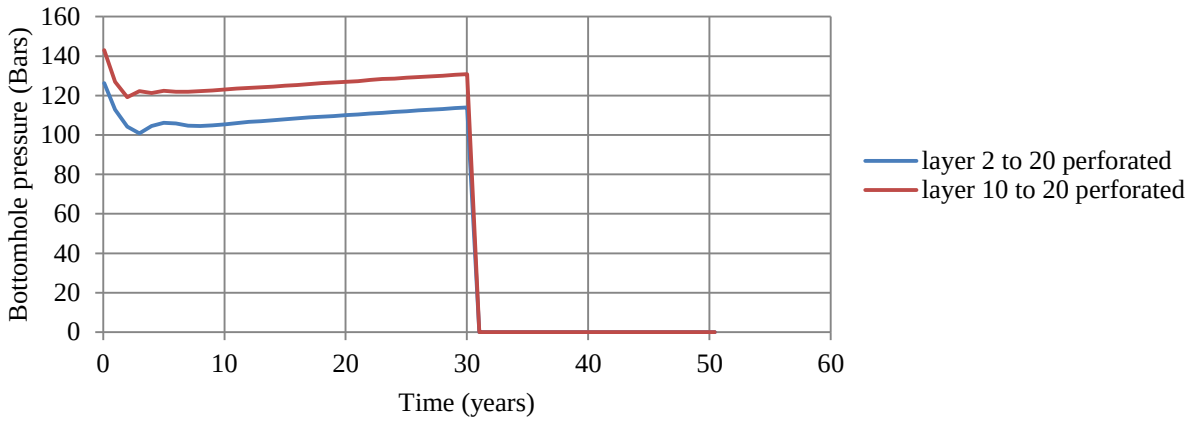

Figure D.18 - Bottomhole pressure from perforation interval variation.

Appendix D.6 Horizontal Permeability

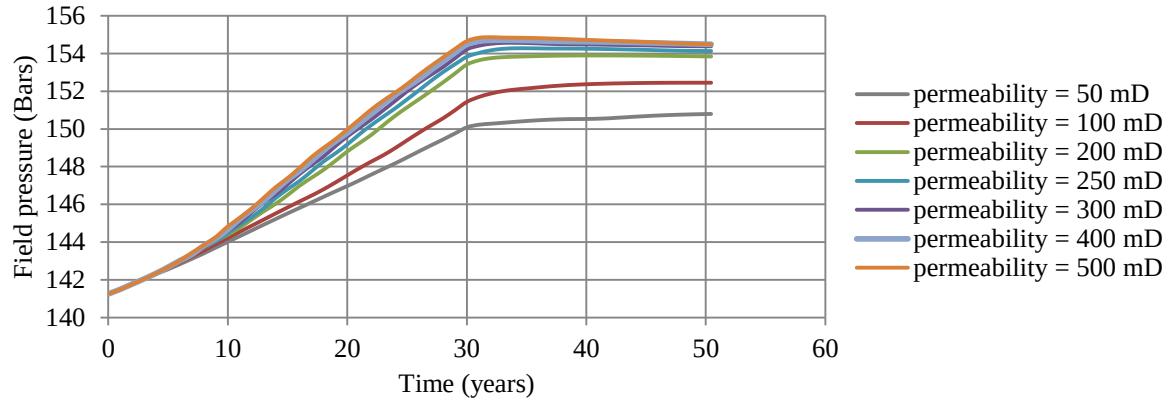

Figure D.19 - Field pressure from horizontal permeability variation.

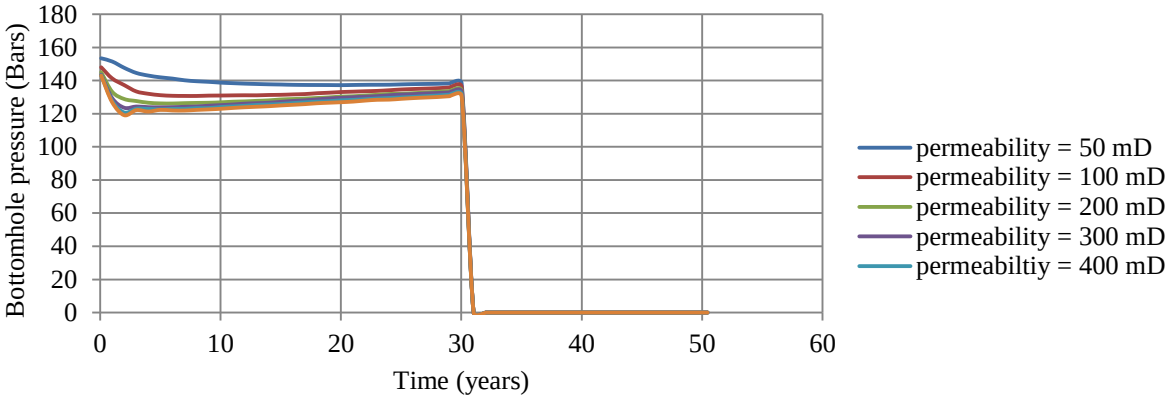

Figure D.20 - Bottomhole pressure from horizontal permeability variation.

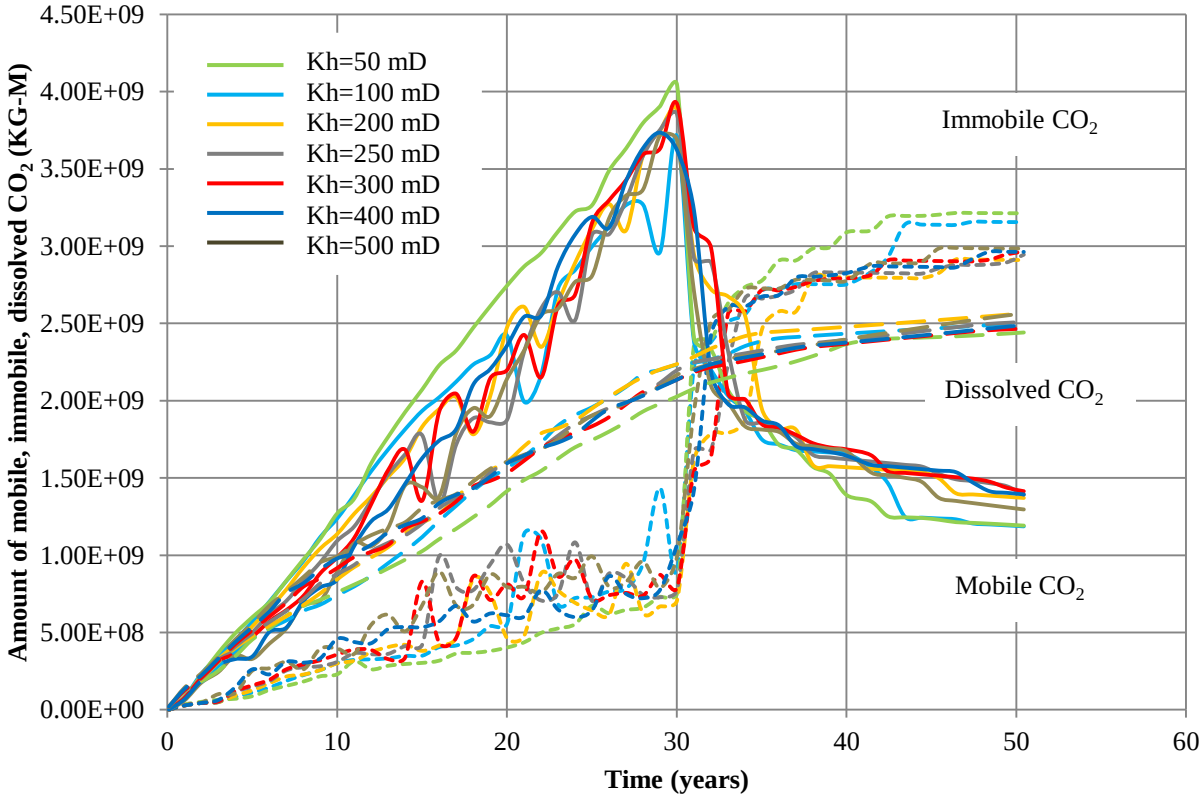

Figure D.21 - CO_2 phase distribution from horizontal permeability variation.

Appendix E. Simulation code

```
RUNSPEC

METRIC

OPTIONS3
  7* 1 /

DIFFUSE

COMPS
 3 /

DIMENS
 140 110 20 /

TABDIMS
 4 1 40 40 /

WELLDIMS
 20  /

CO2STORE

FULLIMP

SATOPTS
  HYSTER  /

START
 1 JAN 2011 /

UNIFOUT
UNIFIN

--Grid section------------------------------------------------------

GRID

DX
 308000*500 /

DY
 308000*500 /

DZ
 308000*63    /

TOPS
 15400*1717 /

PORO
 308000*0.18 /

PERMX
  15400*0.001
  15400*500
  15400*500
  15400*500
```

```
  15400*500
  15400*500
  15400*500
  15400*500
  15400*500
  15400*500
  15400*500
  15400*500
  15400*500
  15400*500
  15400*500
  15400*500
  15400*500
  15400*500
  15400*500
  15400*500
   /

COPY
 PERMX PERMY /
/

PERMZ
  15400*0.0001
  15400*50
  15400*50
  15400*50
  15400*50
  15400*50
  15400*50
  15400*50
  15400*50
  15400*50
  15400*50
  15400*50
  15400*50
  15400*50
  15400*50
  15400*50
  15400*50
  15400*50
  15400*50
  15400*50
   /

INIT

--Properties section--------------------------------------------

PROPS

CNAMES
  'H2O' 'CO2' 'NACL'   /

ZMFVD
 1750  0.99454  0  0.00546 /

DIFFCWAT
0.0001   0.0001  0.0001
/
```

```
DIFFCGAS
0.001 0.001  /

RTEMP
 62.8 /

WSF
0.423    0
0.452    0.0059
0.481    0.019
0.51     0.038
0.538    0.0622
0.567    0.0912
0.596    0.1248
0.625    0.1628
0.654    0.205
0.683    0.2512
0.711    0.3014
0.74     0.3553
0.769    0.413
0.798    0.4743
0.821    0.5392
0.856    0.6076
0.885    0.6794
0.913    0.7546
0.942    0.8332
0.971    0.915
1        1        /

0.423    0
0.452    0.0059
0.481    0.019
0.51     0.038
0.538    0.0622
0.567    0.0912
0.596    0.1248
0.625    0.1628
0.654    0.205
0.683    0.2512
0.711    0.3014
0.74     0.3553
0.769    0.413
0.798    0.4743
0.821    0.5392
0.856    0.6076
0.885    0.6794
0.913    0.7546
0.942    0.8332
0.971    0.915
1        1        /

0.423    0
0.437    0.001
0.451    0.0036
0.465    0.0079
0.479    0.0141
0.493    0.022
0.507    0.0317
0.521    0.0432
```

0.535 0.0566
0.549 0.0719
0.563 0.089
0.577 0.108
0.591 0.1288
0.605 0.1516
0.619 0.1763
0.633 0.2029
0.647 0.2314
0.661 0.2618
0.675 0.2941
0.689 0.3284
0.703 0.3646 /

0.423 0
0.437 0.001
0.451 0.0036
0.465 0.0079
0.479 0.0141
0.493 0.022
0.507 0.0317
0.521 0.0432
0.535 0.0566
0.549 0.0719
0.563 0.089
0.577 0.108
0.591 0.1288
0.605 0.1516
0.619 0.1763
0.633 0.2029
0.647 0.2314
0.661 0.2618
0.675 0.2941
0.689 0.3284
0.703 0.3646 /

GSF
0 0 0
0.029 0.0002 4.6239
0.058 0.0006 5.8072
0.087 0.0015 6.6985
0.115 0.0031 7.4434
0.144 0.0055 8.1566
0.179 0.009 8.9847
0.202 0.0138 9.5266
0.231 0.0199 10.222
0.26 0.0276 10.949
0.289 0.037 11.722
0.317 0.0484 12.533
0.346 0.0619 13.468
0.375 0.0776 14.535
0.404 0.0957 15.794
0.433 0.1163 17.340
0.462 0.1398 19.341
0.49 0.166 22.034
0.519 0.1954 26.461
0.548 0.2279 35.874
0.577 0.2638 /

0 0 0

```
0.029    0.0002   3269.6068
0.058    0.0006   4106.3395
0.087    0.0015   4736.5960
0.115    0.0031   5263.2852
0.144    0.0055   5767.6433
0.179    0.009    6353.1927
0.202    0.0138   6736.3807
0.231    0.0199   7228.7337
0.26     0.0276   7742.1276
0.289    0.037    8289.0174
0.317    0.0484   8862.8073
0.346    0.0619   9523.3544
0.375    0.0776   10278.270
0.404    0.0957   11168.587
0.433    0.1163   12261.276
0.462    0.1398   13676.826
0.49     0.166    15580.637
0.519    0.1954   18711.312
0.548    0.2279   25367.263
0.577    0.2638            /

0.297    0        11.9468
0.311    0.0001   12.3535
0.325    0.0003   12.7807
0.339    0.0005   13.2320
0.353    0.0009   13.7117
0.367    0.0017   14.2249
0.381    0.0029   14.7780
0.395    0.0048   15.3788
0.409    0.0077   16.0373
0.423    0.0119   16.7665
0.437    0.0176   17.5837
0.451    0.0253   18.5126
0.465    0.0354   19.5864
0.479    0.0483   20.8541
0.493    0.0645   22.3917
0.507    0.0846   24.3243
0.521    0.1091   26.8781
0.535    0.1386   30.5183
0.549    0.1737   36.4258
0.563    0.2152   49.1495
0.577    0.2638            /

0.297    0        8447.6823
0.311    0.0001   8735.2581
0.325    0.0003   9037.3416
0.339    0.0005   9356.4742
0.353    0.0009   9695.6728
0.367    0.0017   10058.577
0.381    0.0029   10449.651
0.395    0.0048   10874.463
0.409    0.0077   11340.094
0.423    0.0119   11855.734
0.437    0.0176   12433.600
0.451    0.0253   13090.389
0.465    0.0354   13849.678
0.479    0.0483   14746.136
0.493    0.0645   15833.373
0.507    0.0846   17199.925
0.521    0.1091   19005.704
```

```
0.535     0.1386   21579.699
0.549     0.1737   25756.991
0.563     0.2152   34753.977
0.577     0.2638             /

EHYSTR
  1*  4  2*  KR /

ROCK
 225  1.5E-5 /

--Region section------------------------------------------------------
REGIONs

SATNUM
308000*1  /

IMBNUM
308000*2  /

EQUALS
 SATNUM 2 1 140 1 110 1 1 /
 IMBNUM 4 1 140 1 110 1 1 /
/

--Solution section----------------------------------------------------

SOLUTION

 EQUIL
 3200 225 0.0 0 0.0 0   /

RPTRST
 RESTART PRESSURE SGAS SWAT DENG DENW VGAS VWAT XMF AQSP AQPH  /

RPTSOL
 PRESSURE SGAS SWAT DENG DENW VGAS VWAT XMF AQSP AQPH  /
/

SUMMARY    ============================================================

FPR
FGIPL
FGIPG

BPRES
70 55 10 /
71 55 10 /
72 55 10 /
73 55 10 /
74 55 10 /
75 55 10 /
76 55 10 /
77 55 10 /
78 55 10 /
/

WBHP
 'CO2_INJ'
 'CO2_INJ2'
```

```
 'CO2_INJ3'
 'CO2_INJ4'
 'CO2_INJ5' /

FGIR

WGIR
 'CO2_INJ'
 'CO2_INJ2'
 'CO2_INJ3'
 'CO2_INJ4'
 'CO2_INJ5' /

FWCD
FGCDI
FGCDM
FGIT

RUNSUM

--Schedule section---------------------------------------------------------

RPTONLY
SCHEDULE

RPTSCHED
 PRESSURE SGAS SWAT DENG DENW VGAS VWAT XMF AQPH  /

WELSPECS
 'CO2_INJ' 'FIELD' 70 55 1750 'GAS' 1*  /
 'CO2_INJ2' 'FIELD' 35 23 1750 'GAS' 1*  /
 'CO2_INJ3' 'FIELD' 105 78 1750 'GAS' 1*  /
 'CO2_INJ4' 'FIELD' 35 78 1750 'GAS' 1*  /
 'CO2_INJ5' 'FIELD' 105 23 1750 'GAS' 1*  /
/

COMPDAT
 'CO2_INJ' 70 55 10 20  'OPEN' 1* 1* 1* 2*  /
 'CO2_INJ2' 35 23 10 20  'OPEN' 1* 1* 1* 2*  /
 'CO2_INJ3' 105 78 10 20  'OPEN' 1* 1* 1* 2*  /
 'CO2_INJ4' 35 78 10 20  'OPEN' 1* 1* 1* 2*  /
 'CO2_INJ5' 105 23 10 20  'OPEN' 1* 1* 1* 2*  /
/

WELLSTRE
 'SeqCO2' 0.0 1.0 /
/

WINJGAS
 'CO2_INJ' STREAM 'SeqCO2' /
 'CO2_INJ2' STREAM 'SeqCO2' /
 'CO2_INJ3' STREAM 'SeqCO2' /
 'CO2_INJ4' STREAM 'SeqCO2' /
 'CO2_INJ5' STREAM 'SeqCO2' /
/

WCONINJE
 'CO2_INJ' 'GAS' 'OPEN' 'RATE' 2960000 /
 'CO2_INJ2' 'GAS' 'OPEN' 'RATE' 2960000  /
 'CO2_INJ3' 'GAS' 'OPEN' 'RATE' 2960000  /
```

```
 'CO2_INJ4' 'GAS' 'OPEN' 'RATE' 2960000  /
 'CO2_INJ5' 'GAS' 'OPEN' 'RATE' 2960000  /
/

DATES
1 'FEB' 2011 /
1 'JAN' 2012 /
1 'JAN' 2013 /
1 'JAN' 2014 /
1 'JAN' 2015 /
1 'JAN' 2016 /
1 'JAN' 2017 /
1 'JAN' 2018 /
1 'JAN' 2019 /
1 'JAN' 2020 /
1 'JAN' 2021 /
1 'JAN' 2022 /
1 'JAN' 2023 /
1 'JAN' 2024 /
1 'JAN' 2025 /
1 'JAN' 2026 /
1 'JAN' 2027 /
1 'JAN' 2028 /
1 'JAN' 2029 /
1 'JAN' 2030 /
1 'JAN' 2031 /
1 'JAN' 2032 /
1 'JAN' 2033 /
1 'JAN' 2034 /
1 'JAN' 2035 /
1 'JAN' 2036 /
1 'JAN' 2037 /
1 'JAN' 2038 /
1 'JAN' 2039 /
1 'JAN' 2040 /
1 'JAN' 2041 /
/

WELLSHUT
'CO2_INJ' /
'CO2_INJ2' /
'CO2_INJ3' /
'CO2_INJ4' /
'CO2_INJ5' /
 /

DATES
1 'JAN' 2042 /
1 'JAN' 2043 /
1 'JAN' 2044 /
1 'JAN' 2045 /
1 'JAN' 2046 /
1 'JAN' 2047 /
1 'JAN' 2048 /
1 'JAN' 2049 /
1 'JAN' 2050 /
1 'JAN' 2051 /
1 'JUN' 2052 /
1 'JUN' 2053 /
1 'JUN' 2054 /
```

```
1 'JUN' 2055 /
1 'JUN' 2056 /
1 'JUN' 2057 /
1 'JUN' 2058 /
1 'JUN' 2059 /
1 'JUN' 2060 /
1 'JUN' 2061 /
/

END
```